



CGU HS Committee on River Ice Processes and the Environment
13th Workshop on the Hydraulics of Ice Covered Rivers
Hanover, NH, September 15-16, 200

Instrument for Detecting Freeze-up, Mid-Winter and Break-up Ice Processes in Rivers

Martin Jasek

BC Hydro, Burnaby, BC, martin.jasek@bchydro.com

John Marko, David Fissel, Murray Clarke and Jan Buermans

*ASL Environmental Sciences Inc., Sidney, BC, jmarko@aslenv.com dfissel@aslenv.com,
mclarke@aslenv.com, jbuermans@aslenv.com*

Kerry Paslawski

Timberroot Environmental, Beaverlodge, AB, timberrt@telusplanet.net

A new underwater acoustic instrument for river ice studies has been designed, developed, and deployed in the Peace River in Northern Alberta, which is hydraulically regulated by upstream hydroelectric projects. The data is being collected to support studies related to ice jam occurrences and hydropower operations during the winter.

An upward looking sonar instrument was deployed for the 2004-2005 ice season. From the acoustic backscatter returns of the transmitted acoustic pulses, the sonar instrument measured the distance to the water surface or the underside of floating ice at the surface. The instrument also had the capability to record the profile of acoustic backscatter returns through the river water column.

The instrument provided valuable insights into numerous freeze-up, mid-winter and spring ice processes difficult or impossible to obtain by other methods. These processes included formation of frazil in suspension, development of frazil ice pans, anchor ice formation/detection, formation of the river ice cover including highly dynamic freeze-up events, changes in the river ice cover over the winter, undercover ice transport and, finally, thermal break-up.

1.0 Introduction

The Peace River in northern British Columbia and Alberta is regulated by the WAC Bennett and Peace Canyon dams (Figure 1.1.1). During the winter, flow releases have to be managed to reduce the potential for ice jamming and subsequent flooding that can occur under a variety of environmental conditions. At particular risk is the Town of Peace River, Alberta about 375 km downstream from the hydroelectric facilities. These management efforts require better understandings of river ice processes, including calibration of computer ice models. The collection of field data is useful for meeting these management requirements as well as for providing baseline data for ongoing evaluations and for assessing potential development of the Dunvegan Hydroelectric Project about 100 km upstream of the Town of Peace River.

The Shallow Water Ice Profiling Sonar (SWIPS) unit, which was central to 2004-2005 field measurement campaign, was deployed near the Town of Peace River (Figure 1.1.1) to investigate ice processes at a location where such processes could have near-maximal impact on overall Peace River management. The chosen site was also logistically convenient, as close proximity to the town site allowed for both frequent site visits and use of other data being collected in surrounding areas.

1.1 Measurement Objectives

Measurements of ice processes occurring in the water layer and/or below the uppermost ice surface have been rarely reported upon in the literature for obvious reasons, especially corresponding to times when the ice is moving or too dangerous to support personnel. The SWIPS was deployed to fill the resulting gaps in knowledge of dynamic winter river environments. Specific targets of the SWIPS measurement effort were the elusive processes involved with: suspended frazil ice, formation of ice pans and the seasonal ice cover; and the changes, including break-up, which occur in the latter seasonal feature. Near-continuity of SWIPS measurements, even during the winter season when on-ice field measurements were feasible, was to be maintained to allow recording of changes due to erosion, deposition and ice transport.

Other measurement objectives were directed at determining the capabilities of the new SWIPS instrument. This instrument evolved from the well established Ice Profiling Sonar (IPS) instrument which has been used, for more than a decade, to measure sea ice drafts during long deployments in the world's polar and sub-polar oceans. The IPS provides recorded measurements of upward-looking ranges to the sea ice undersurface which can be combined with high precision water level data to allow detailed sampling (0.1 to 1 Hz) of sea-ice draft (the underwater portion of ice thickness) (Melling et al., 1995; Birch et al., 2000; Fissel et al., 2004). A real-time output version of the IPS was first developed in 2000-2001 for use on the lower St. Lawrence River (Morse et al., 2003; Chave et al., 2004). The present study was intended to demonstrate the first field use of the SWIPS instrument which differs from the IPS instrument in four key respects: (a) the instrument is designed for use in shallow water where usage of much less expensive acoustic transducers and pressure sensors is feasible; (b) the instrument is configured so that nearly all electronic and instrument housing components are onshore, reducing costs and risks of equipment damage and loss and providing real-time access to measurement parameters and results; (c) the instrument includes a profiling measurement mode

on selected samples (pings) additional to the traditional target (ranging) operational mode, which allows for collection of information on the internal structure/contents of the ice layer and the underlying water column; and (4) the study represents the first use of IPS technology for measurement of river ice. The collected data, supported by ancillary and independent field measurements provide a basis for detailed evaluation of the utility of the SWIPS instrument for river ice studies.

1.2 Overview of the Ice Season

Figure 1.2.1 shows the positions of the leading edge of the stationary ice cover (ice front) over a 600 km length of the Peace River during the 2004-2005 ice season. Also shown are the location of the SWIPS and the hourly temperature record in the river valley at a location about 7 km away from the SWIPS site (Figure 1.1.1). On a macroscale basis, the freeze-up process was judged to be typical of other years.

The first period of cold weather (defined as an extended interval of air temperature well below freezing) occurred at the beginning of December, producing surface ice floes as well as suspended ice in the water column. At the time, the ice front was several hundred km downstream of the SWIPS site. Three above-freezing warm spells in December delayed the upstream progression of the ice front and caused episodic cessation of ice floes and suspended frazil appearances at the SWIPS site.

The ice front arrived at the SWIPS location on Jan. 6, compressing, shoving and thickening a mixture of floes and slush ice before advancing to a position 5 to 10 km upstream of the SWIPS.

A major consolidation occurred at approximately 04:00, Jan. 7, as the ice cover at the SWIP site mobilized and travelled downstream. This event ended at about 07:15 that day and a new and more stable ice cover formed over the SWIPS site which remained in place for the remainder of the ice season. Although similar destabilization/stabilization events occur every year somewhere on the river, they are localised and therefore relatively rare at any particular location. The last time an event of a similar magnitude occurred near the SWIPS site was in 1992.

A warm spell during the first two weeks of March produced snowmelt in the unregulated part of the river basin, greatly increasing river discharges and water levels. This change also caused the ice front to recede rapidly downstream. However, cooler weather in the third week of March delayed further recession of the ice front; in fact, advancing the ice front upstream. Warmer weather returned in the last week of March and persisted through April. However, depletion of the prairie snowpack by a previous warm spell prevented a subsequent large increase in run-off and water levels remained low. The mild weather did, however, produce warming in river water upstream of the ice front which eventually initiated thermal break-up of the ice cover at the SWIPS site at about 03:00 on Apr 3.

On April 4 Alberta Environment staff observed (Granson et al., 2005a) pieces of ice on the river banks were observed being released in the area upstream of the ice front and travelling downstream. This ice would have subsequently moved past (and over) the SWIPS site.

2.0 Plan and Measurement Methods

2.1 Instruments: Deployment and Operation

A shallow Water Ice Profiling Sonar (SWIPS) instrument was deployed on November 3, 2004 to obtain river ice measurements near the town of Peace River Alberta (see Figure 1.1.1). The SWIPS unit was manufactured by ASL Environmental Sciences Inc. and was designed to extend the Company's widely-used deepwater marine ice-profiling technology to provide near-real-time measurements for shallow water applications where shore-based power, control and data display/storage facilities are available.

The basic in-water elements of the SWIPS (Figure 2.1.1) were a 235 kHz transducer, two tilt-sensors (measuring about orthogonal horizontal axes) and a temperature sensor which were powered and linked to a sheltered onshore control and data storage unit (Figure 2.1.1) with a total capacity of 64 Mbytes of flash memory. More information on the instrument specifications are provided in Table 2-1. A Solinst internal recording pressure/temperature sensor was also mounted on the cement anchor, adjacent to the SWIPS to provide hydrostatic pressure data. The latter pressure measurements, in conjunction with atmospheric pressure data, allow determinations of local river water levels. Subtraction of the SWIPS-measured acoustic ranges (distance from the ice under-surface to river bottom) from such water levels yields values of underwater thickness or draft for the river ice.

The acoustic frequency of 235 kHz, which allows detection of discrete targets with diameters at least as small as 6 mm was used to both provide this capability and, as well, to allow some penetration of diffuse ice features (such as slush ice). For specific detection and measurements of small ice crystal structures, such as frazil ice during initial formation and/or in low concentrations, it may be advantageous to use still higher frequencies since the minimum detectable particle size should scale, roughly, as the inverse of the acoustic frequency.

A feature of the 2004-2005 monitoring program was its utilization of the SWIPS capacity for operations in both target ranging and profiling modes. For the target ranging mode, the instrument provides a single range value for each acoustic transmission, or ping, that represents the acoustic range to the closest portion of the ice undersurface on the basis of exceedance of a specified threshold of return signal amplitude. Such measurements were carried out at a high sampling frequency (1Hz). Profiling mode measurements were carried out less frequently, i.e. at intervals no shorter than 12 seconds, because of the much larger amounts of data acquired corresponding to individual ping amplitudes sampled at roughly 29.8 kHz. Profile outputs correspond to return amplitudes associated with segments of the water column with vertical dimension of, roughly, 2.4 cm. In the 5 to 8 m water depths and with the 1-2 m thick ice characteristic of the Peace River site, the 10 degree beam of the SWIP transducer insonified circular portions of the water-air or water-ice interfaces with diameters ranging between, approximately, 0.8 and 1.6 m.

The SWIPS capability to support downloading of data by field crews with computer access to the shore-based electronics, provided the opportunity for near-realtime data access for monitoring instrument performance and changing key sampling parameters to assure optimized information collection. Over the course of the measurement program from November 2004 to April 2005,

the instrument was operated continuously, with a total of 18 different files, or data sets, being downloaded. The sampling parameters used for the various data sets are summarized in Table 2-2. Prior to the consolidation of the river ice in early January, instrument gain settings were increased and the threshold level for target detection lowered. These changes were made to both improve detection of frazil ice in the river and to attempt to overcome episodic signal fading arising from formation of anchor ice on the transducer. Later in the program, the burst sampling rate was increased, in stages, from 25 pings every 30 minutes to once every 12 seconds, in order to obtain improved time resolution of ice features on the bottom of floating river ice and to detect episodic occurrences of ice particles moving below such ice. The results of the sampling parameter changes are reflected in the acoustic results presented in Section 3.

Table 2-1: Instrument Specifications for the Shallow Water Ice Profiling Sonar (SWIPS)

Power requirements:	8 to 18 V and 50 mA max current draw continuously.
Range:	1 to 10 m (3 to 33 ft)
Water Temperature:	0 to 4 °C ± 1 °C and 4 to 10 °C ± 2 °C
Tilt Useful range:	± 75 degrees on both axes.
Tilt Accuracy:	± 1° over the range of ± 15 degrees on both axis
Accuracy on range:	±0.05 m (2 inches). The accuracy of the ice draft depends on the existing water level sensor.
Standard output signal:	RS-232
Ambient temperature:	-40 to 40 degrees C (or -42 to 106 deg F). Surface panel must be shielded from direct sunlight.
Underwater components:	Underwater cable and sensor are deemed disposable in case of ice impacts. The underwater cable length is specified at time of order according to user requirements.
Transducer mounting:	The sensor needs to be positioned within ± 15 degrees of vertical. Transducer tilt should be verified at deployment. Mounting design assistance and equipment is available upon request. The transducer mount should be placed to minimize effects from ice impact.

Table 2-2: Summary of the key SWIPS sampling parameters used for each of the 18 data sets obtained.

Data Set Number	1-3	4	5-8	9	10	11-12	13-14	15-18
Start Date	20041104	20041213	20041214	20041222	20041230	20050105	20050119	20050120
Stop Date	20041213	20041214	20041222	20041230	20050105	20050119	20050120	20050415
Gain Setting (1=low 4= high)	3	4	4	4	4	4	4	4
Target Threshold Amplitude	200	200	80	40	40	40	40	40
Target Sampling Interval (s)	1	1	1	1	1	1	1	1
Burst Interval (s)	1800	1800	1800	1800	3600	3600	60	12
No of Samples Each Burst	25	25	25	25	120	25	1	1

Post processing of the SWIPS data was limited to editing the range data using automated and manual review methods. The acoustic range values were also adjusted to allow for the effects of changes in the speed of sound of the river water when the river water was not at the constant

assumed value of 1402.3 m/s (the freezing point value) on the basis of Solinst temperature measurements. Subsequently, a review of the ice drafts during open water periods showed that the speed of sound corrections were very reasonable and no further modifications were required.

2.2 Supporting field measurements

Measurements of frazil ice pan thicknesses were carried out with an underwater video camera mounted on an L-shaped boom, the vertical portion of which included scale graduations that could be read when the camera was positioned at the bottom of the ice pan. Unfortunately, the field crew was only available to make these measurements during periods when anchor ice was blocking the SWIPS signals, precluding direct comparisons with SWIPS-measured ice drafts.

Three manual ice measurement surveys were conducted over the SWIPS deployment location on Jan. 19, Feb. 3 and Mar. 2 with each survey utilizing a seven-hole measurement grid. Relative to the SWIPS deployment site: hole #1 was about 3 m upstream; hole #2 was 3 m further out from the bank; hole #3 was over the deployment site; hole #4 was 3 m closer to the bank; hole #5 was 3 m downstream; hole #6 was 6 m downstream; and hole #7 was 9 m downstream. The concentration of holes downstream of the SWIPS site reflected the suspicion that the instrument had moved downstream due to anchor ice attachment early in the deployment. Individual hole drilling efforts in successive field programs were not carried at identical locations but utilized small displacements of less than 1m to ensure all obtained data were representative of undisturbed portions of the ice cover. Actual drilling was carried out with a 0.20 m diameter power auger. Thermal ice thickness was measured on opposing sides of each hole with a graduated stick and a mounted horizontal bar and the two obtained measurements averaged to yield a mean hole value. The total ice thickness (to the bottom of the slush layer) was measured with an underwater video camera mounted at the end of a graduated pole. The results of the field surveys are shown in Figure 2.1.2.

To investigate possible movements in central portions of the slush layer suggested by profile data, sticks on strings were inserted into this layer through the measurement holes and observed over periods of several hours. No movements internal to the slush layer were detected with this methodology.

The SWIPS/Solinst unit was recovered on Apr 15, 2005 with the aid of a jet boat. There was a significant amount of woody debris on the communications/mooring cables but no damage to the cables or to the SWIPS was detected. Although the exact position of the SWIPS unit relative to its deployment location was difficult to determine, it was in the same general area (within 10 m) as the original deployment site, indicating that the anchor ice did not move the SWIPS unit substantially.

3.0 Results

3.1 Pre-Freeze-up and Initial Ice Formation

Figure 3.1.1a shows water temperatures at the SWIPS site during the period associated with episodically interspersed local occurrences of ice floes and open water. These temperatures first fell below the freezing point just before noon on Dec. 6, 2004. SWIPS profile data for Dec. 6-7 as well as corresponding water levels and water temperatures measured by the Solinst instrument are plotted in Figure 3.1.2 with a specific delineation of the timing of the transition from

temperatures above 0 °C to below 0 °C. It is evident that a sudden increase in mid-water column targets and surface ice floes was detected within a fraction of an hour after supercooling was achieved. The numbers and thickness of the ice floes on the river surface increased with time, coincident with decreases in concentrations of the suspended targets. This combination of trends is consistent with the theoretical expectations of Lal and Shen (1991) and Andres (1995) who showed that the additional insulation of underlying river waters produced by increasing concentrations of surface ice reduces supercooling and, hence, frazil ice generation. This effect, in turn, reduces the numbers and sizes of the frazil ice particles appearing in the water column.

Figures 3.1.3a and 3.1.3b display portions of the same data at full resolution (1 second profiles) for the first suspended ice- and frazil pan-dominated periods respectively. These results demonstrate that the SWIPS has potential for offering quantitative measures of suspended ice concentrations as well as of surface ice pan concentrations, floe sizes and thicknesses. Typical floes (or frazil pans) on the Peace River are shown in Figure 3.1.4.

Figure 3.1.1a also shows that, starting early on Dec. 7, the SWIPS return signal began to fade, becoming completely absent by the end of the day. Formation of anchor ice around the unit, which blocked the acoustic signal, was the suspected cause of this signal loss. Independent confirmation of this interpretation was obtained during a later, December 12-16, portion of the signal loss interval when the plotted tilt sensor and water level-based elevation data were suggestive of significant movements of the SWIPS/Solinst unit along the river bottom (Figure 3.1.1b). Apparently, the buoyancy of the anchor ice accretions was sufficient to allow downstream drift of the unit to a location that was approximately 0.5 m shallower than the original deployment site. There was no change in water velocities during this time sufficient to explain the movement which was only detected during this first of several incidents of supercooling and anchor ice formation. A possible explanation for the absence of similar movements in later anchor ice episodes is that the steel cable mooring the unit to the shore had been stretched to its limit by the movements of the first episode, precluding further downstream drift. Evidently, the anchor ice was removed from the SWIPS unit during the warming trend initiated on Dec.16, allowing resumption of range and profile data collection.

A return to supercooled water temperatures gave rise to additional mid-water column and surface ice targets early on Dec. 22 (Figure 3.1.5a) and, eventually, produced further blockage of the unit's signal for most of Dec. 23. A warm spell caused water temperatures to rise above freezing on Dec. 25 and 26, allowing the reappearance of ice targets on Dec. 27. The December 27 to 30 period was the longest interval during in which ice floe data were recorded by the SWIPS without interruptions by anchor ice accumulation. There was some evidence of signal weakening on Dec 29 (Figure 3.1.5a) attributable to such an accumulation. It is interesting that the latter parts of both this time interval and the Dec. 23 signal blockage interval were associated with very strong returns from portions of the water column immediately above the SWIPS unit. It is likely that, in both cases, the latter returns were from anchor ice as it cleared from the monitoring site.

Figure 3.1.5b represents data at slightly higher temporal resolution as recorded during the Dec. 27 period associated with high concentrations of suspended ice targets. Peak concentrations were evident in the first three hours after supercooling followed by a gradual decline to only sporadic

ice target occurrences 12 hours after supercooling. The Figure also shows that there appeared to be a larger number of targets in proximity to the river bed as opposed to the upper part of the water column. This difference may be indicative of preferential frazil formation in the vicinity of the river bottom and its adjacent elevated concentrations of suspended sediments which provide favourable sites for frazil crystallization from turbulently-mixed supercooled water (Daly and Ettema, 2005). Figure 3.1.5b also shows that the frazil ice pan drafts increased to about 0.6 m over this period with some drafts exceeding 1 m.

Figure 3.1.5c presents snapshots of full resolution profile data spanning about 36 hours from Dec. 27, 02:47 to Dec. 28, 14:47. These figures show frazil pan evolution with time, revealing increases in number, surficial coverage and thickness of the ice floes. Although outside of the scope of this paper, it should be possible to quantify the latter parameters from the obtained data. Figures 3.1.5b,c also display the decreasing strength of mid-water column ice targets (suspended frazil ice) over the included time period.

3.2 Ice Cover Formation and Dynamic Winter Events

At 10:10 Jan. 5, 2005, the ice front was about 15.6 km downstream of the SWIPS location (Granson et al. 2005a) and advancing rapidly under a cooling weather trend. This advance started to raise the water level at the SWIPS site due to a backwater effect beginning on the evening of Jan. 5 (Figure 3.2.1). The ice front advance towards the SWIPS location continued from Jan. 5 to 6 with a minor retreat or consolidation being noted late on Jan. 5 in the form of a drop in local water levels. Although not directly observed, estimates from the water level record suggest that the ice front reached the SWIPS location at about 06:00, Jan. 6. Interestingly, although the SWIPS unit had been covered by anchor ice since Dec 30, this obstruction was cleared shortly after the apparent ice front arrival (10:42, Jan. 6). The subsequently measured acoustic ranges to the ice undersurface, as adjusted to geodetic datum, are plotted in Figure 3.2.1 along with the water level elevations as measured both at the SWIPS site and at the Water Survey of Canada gauge in the Town of Peace River about 6.9 km downstream. The occurrences of some SWIPS targets above the indicated water levels can be explained by multiple reflections or reverberation arising from back-scattering at the rough ice undersurface which introduce deviations from the nominally vertical sonar signal paths. These deviations increased overall signal travel times and, hence, the apparent measured ranges. In fact, observations of numerous null targets suggest that some sonic pings were scattered with deviations from the vertical large enough to escape detection (see null data points at elevations near 309.6 m in Figure 3.2.1).

Ice cover stabilization at the SWIPS site (Jan. 6-7) incorporated three distinct episodes of consolidation (11:10-12:20 and 17:05-17:45, Jan.6; and 04:00-07:15, Jan. 7). These episodes were separated by intervening periods during which the ice cover was stationary and of approximately constant thickness. Although the target range data for the stationary ice cover did show some scatter, this scatter or “noise” in the target ranges was present for the remainder of the ice season and will be discussed again in Section 3.3.

After the first recorded consolidation event, the ice formed a relatively thin cover of less than 1 m thickness. The second consolidation produced an ice cover with a thickness slightly in excess of 2m. The third, last, and largest event in the sequence moved this ice downstream and brought

a new ice cover over the site with thicknesses of just under 2 m. Due to its magnitude, this latter event is of particular interest and will be discussed in some detail.

Figure 3.2.2 shows the individual draft values measured during this (Jan. 7) event were characterized by high variability and ranged upward from zero to in excess of 6 m. Figure 3.2.3 shows this same data plotted relative to the geodetic datum along with water levels as measured at the SWIPS site and 6.9 km downstream. Even at this moderate display time scale, it is difficult to extract ice structural details from the 1-second sampling interval ranging data. Figure 3.2.3 also delineates the measurement times associated with successive collections of 25 seconds of profile data at hourly intervals (red lines). Figure 3.2.4 shows these successive hourly sets of 25 profiles plotted adjacently along with corresponding water level values. The first panel in the Figure corresponds to a stationary ice cover period, while the middle three panels display data from the event's consolidation phase. The last panel shows the ice cover after it has returned again to stationary conditions. It is evident from the second panel that even the deepest returns were not derived from suspended ice particles but, rather, were associated with sustained (for at least 25 seconds in this case) ice draft targets suggestive of macroscale ice features. To obtain some insight into the size of these features, Figure 3.2.5 displays 8 minutes of the 1-second interval target elevation data recorded during a period of maximal ice thicknesses spanned by the 3.25 hour duration consolidation event. Superimposed on the plot is the second panel of profile data from Figure 3.2.4. This figure shows that deep macroscale ice features were common during the event.

3.3 Changes to Winter Ice Cover and Under Cover Ice Transport

Figure 3.3.1 shows the 12-hour means of ice drafts for the entire season, as well as the indicated, related, statistical quantities. It can be seen that, from Jan. 7 to Mar. 5, ice drafts decreased more or less monotonically from 1.90 m to 1.63 m, giving an average rate of decrease of 4.7 mm/day. By Apr. 1 the ice draft was about 1.31 m giving an average rate of decrease of 11.9 mm/day for the Mar. 5 to Apr. 1 period. The thinning rate, thus, increased considerably in the latter part of the ice season. It should also be noted that the overall spread of draft estimates at a given time, as indicated, for example, by the difference between plotted 99 and 1 percentile individual draft samples, increased and remained at higher levels beginning on about February 23. Further understandings of the overall trends shown in Figure 3.3.1 can be obtained from reviews of the corresponding SWIPS profile data plotted in Figure 3.3.2.

Such reviews are facilitated by the inclusion in the Figure of additional data descriptive of the profiled ice and water structures. Key components of this information are the ranges associated with local water levels as determined from the hydrostatic pressure measured at the monitoring site. A second body of data, giving the anticipated range of the slush/thermal ice interface, was plotted utilizing, in part, thermal and total ice thickness information acquired in three field visits (Jan 19, Feb 3, and Mar 2.). Although the latter data were obtained directly above the SWIPS deployment location, the movement of the unit by anchor ice in December, precluded direct comparisons of the manually measured total ice drafts with corresponding SWIPS estimates. However, since thermal ice thickness is known to be a function of air temperature and snow cover which does not vary significantly over short distances, the existing measurements of this parameter can be assumed to be reasonably applicable to the SWIPS site. [This uniformity of thermal ice thickness was confirmed in the March 2 field program which collected data at 3

different arrays of measurement holes separated by distances on the order of 30 m.] Consequently, the differential form of a thermal ice growth equation (Shen and Yapa, 1985) could be used to interpolate and extrapolate the measured thermal thicknesses throughout the full period covered by the data in Figure 3.3.2. With only slight adjustments of nominal coefficient values, the calculated results were found to agree well with the three field-measured mean thermal thickness values. The slush porosity chosen for the calculation was 0.6 after Andres and Van Der Vinnie (2004). Subtraction of the calculated thermal ice thicknesses from the corresponding ranges to the water surface gave the ranges of the thermal/slush ice interface denoted by the narrow yellow-line curve in Figure 3.3.2. Comparisons of the positions of this line relative to the lower edge of the detected ice layer show the presence of pronounced thinning of the slush layer throughout the lifetime of the ice cover. This thinning was also a feature of the manually-obtained data sets which showed an overall decreasing trend but considerable hole to hole slush depth variability on any given date (Figure 2.1.2).

Similar comparisons of the thermal/slush ice interface line with the ranges associated with significant profiling signal return amplitudes also suggest almost complete penetration of the slush layer by the SWIPS acoustic sensing. It is important to note that the latter conclusion is completely dependent upon the implicit assumption of our displayed profiles that the speed of sound in the slush ice layer is identical to that of sound in the underlying water layer. This assumption, while convenient, is, almost certainly incorrect and will be discussed in some detail in Section 3.5 where evidence supporting alternative sound speed assumptions and their implications for internal ice cover sensing will be discussed. Such uncertainties in the physical properties of the lower portion of the ice cover also presently inhibit explanations of the anomalous temporal variations which have been observed in the amplitudes of returns from strong internal ice cover targets. Fluctuations in the apparent ranges and strengths of these targets occur over time scales ranging up to several hours or longer. Potential sources of such variations could arise either from slow movements of harder ice fragments embedded in the slush layer or from time-dependent changes in the lower boundary region of this layer, such as could be associated with movements equivalent to ocean floor sand wave migration. Field evidence appears to favour the latter type of mechanism. Specifically, a video camera placed just below the bottom of the slush layer on Mar. 2 showed frazil and granules up to a few cm in size tumbling along the ice underside as well as numerous ice targets suspended in the water column. The resulting time dependences in the shape and content of the slush/water interface could, through refraction and attenuation, produce alterations in signal returns from the ice cover interior similar to those associated with the observed temporal amplitude variations. The alternative explanation in terms of significant movement within the main body of the slush layer was not supported by the stick and attached string measurement results described in Section 2.2.

Leaving such subtleties aside, Figure 3.3.2 shows that from Jan 7 to Feb 20 the character of the ice cover changed very little, with the observed changes being almost equivalent to the ice cover rising and falling with the water levels. Profiles appeared to indicate the presence of a lowest ice layer with weak (or “soft”) returns characterized by a thickness of a few tens of centimetres, and associated with acoustic backscattering amplitude values in the 0 to 40 count range (blue, green, and yellow in the profile plots). However, after a sudden increase in water levels during the relatively short Feb 20 to Feb 23 period, this softer layer disappeared, being replaced by a more abrupt transition from very low amplitudes to values of 40 or more (blue to red in the plotted

amplitudes). Perhaps not coincidentally, targets in the water column also first appeared on Feb 23 even though similar or even slightly higher water levels were recorded on Feb 20. It is evident that something happened to the bottom of the ice cover during the intervening short period. Neil et al. (1995) indicated that the size of frazil particles at the base of the ice cover could increase from a few millimetres at freeze-up to several centimetres later in the ice-covered season. “Ice pebbles”, typically 3cm and as large as 10cm in size on the Peace River were identified. Similar “frazil pebbles” were observed by Chacho (1986) on the Tanana River in Alaska. Shen and Wang (1995) observed “frazil chips” on the Yellow River. Given the above noted (Section 2) sensitivity of the SWIPS instrument to particles 6 mm or greater in diameter, it is possible the Feb. 23 change in behaviour may represent detection of such a transition to larger granule sizes. A similar transition was noted above in connection with a sudden increase in the spread of measured draft values (Figure 3.3.1). This trend is also graphically evident in the 12-hour averaged profile amplitude profiles of Figure 3.3.3 where the broader (soft ice) profiles from the Jan. 7 to Feb 20 period contrast strongly with the much narrower, later season, “hard ice” profiles (Feb.25 and Mar. 26) which are positioned almost immediately adjacent to the ice undersurface).

Insights into the physical processes responsible for these changes and, more generally, for the thinning of the ice cover at different rates over the course of the winter requires consideration of changing river flows as well as careful examination of the SWIPS profiles. Given the granular nature of the lower ice cover interface, erosion of the lower portion of the slush layer would appear to be the likely cause of the thinning of this layer and of the overall seasonal decrease in total ice draft. The increase in the erosion rate inferred from the March data was an expected consequence of larger river velocities. Increased river flow was precipitated by a substantial warm spell which produced snowmelt run-off in the basin and, consequently, the larger discharges of the Mar. 6 to Mar. 15 period which may be inferred from the higher water levels associated with this period (Figure 3.3.2). Accurate discharges for the ice covered river are not easily obtained but estimates derived from upstream hydrometric station data suggest that discharges increased from about 1600 m³/s to 2100 m³/s during the course of the March 6-15 event. Unfortunately, the absence of water velocity data at the SWIPS site did not allow establishing more quantitative relationships between river flow and ice thinning and suspended ice detection rates. Nevertheless, Figure 3.3.2 provides evidence for a large increase in water column targets for the period Feb. 23 to Mar. 15 which is consistent with increased river flow driving substantial additional volumes of ice particles into suspension. Figure 3.3.4 shows the suspended ice targets at the full 12 second sampling resolution recorded by the SWIPS instrument. Taken together, Figures 3.3.2 and 3.3.4 show that the numbers of detectable target returns in the first 1 or 2 m below the ice cover considerably exceeded the numbers of returns from deeper portions of the water column. This result contrasts strongly with conclusions drawn from upon data collected during the freeze-up period (Figure 3.1.5b) which showed preferential concentrations of suspended ice targets in areas closer to the riverbed. This difference almost certainly reflects the postulated differences in the immediate origins of the frazil particles assumed to be responsible for the respective water column signal returns. Clearly, in the later parts of the ice-covered season most suspended ice particles originate at the slush ice undersurface. The 12-hour average profile for Mar 8 in Figure 3.3.3 corresponding to the period of increased flow shows a slow ramp-up in amplitudes from 0 to 20 counts, which extends downward from the nominal ice undersurface by, roughly, 1 m, reflecting, again, the presence of large amounts of suspended ice particles below the ice undersurface. These concentrations of

suspended ice can be conveniently described as a “cover load”, similar to the “bed load” terminology used in quantifying equivalent modes of sediment transport.

3.4 Thermal Break-up

Figures 3.4.1 and 3.4.2 show SWIPS draft and profile data, respectively, for a period which began about 2 days prior to the, approximately, 03:10, Apr. 3 break-up event and ended a fraction of a day after the end of the event. The first Figure includes a plot of ice drafts and water temperature while Figure 3.4.2 adds information on the calculated true ranges to the bottom of the thermal ice as well as data on water temperature and the positions of the ice front to a display of return signal amplitude profiles.

The plotted data show that, starting at about 00:00 on Apr. 2, water temperatures began to rise with increasing steepness from a time-independent, near-freezing value. The ice cover appeared to thin in response to this change coincident with a detectable increase of suspended cover load. The most rapid thinning occurred at about 12:00 on Apr. 2, followed by, from 12:00 to 14:00, Apr. 2, a substantial decrease in both the cover load and the thinning rate. The ice level at 14:00 coincided with the calculated position of the bottom of the thermal ice: an event which further diminished the weak returns previously noted in connection with the “soft” lower edge of the slush ice. This change is evident in the color-coded profile data of Figure 3.4.2 and, particularly, in the inset plots which show corresponding mean amplitudes versus range data for 30 minute intervals starting, alternatively 1.5 hours before and 0.5 hours after the nominal 14:00 full exposure of the thermal ice undersurface. The plots show this exposure was accompanied by both a small, range increase of several centimeters (notable during a period of slightly decreasing water levels) and the removal of the short range tail or gradual rise in amplitude previously associated with the presence of remnants of the “soft” portions of the slush layer. The lower thinning or melt rate observed at this time would have been consistent with the implied transition from a slush to thermal ice interface and the larger amounts of heat which would have been required to melt the latter ice form. The thermal ice was also likely to be smoother than the rough granular slush interface, thereby further decreasing turbulent heat exchange and the melt rate. The disappearance of the cover load was also indicative of the greater physical stability of a thermal ice undersurface as opposed to its slush ice predecessor. The distances of the ice front from the SWIPS plotted in Figure 3.4.2 for various stages of the break-up period suggest that the thinning process started when the ice front was about 10 to 15 km upstream of the SWIPS and that the slush layer had completely melted when the ice front was still about 6 km away.

The transition from an ice cover to open water, which occurred at about 03:10 on Apr. 3, was abrupt and uneventful. Following the thermal break-up (Apr. 3 to 8) there were many deep-water targets recorded in the 1 Hz range data (Figure 3.4.3). Field observations by Alberta Environment, Granson et al (2005b) indicted that large chunks of shore ice were breaking off and floating downstream on Apr. 4, explaining the detection of deep targets in this period. Some of these could also had been submerged woody debris.

Finally, there was also an increase in suspended targets near the bed during the break-up period (Figure 3.4.2). This increase could be due to woody debris being moved along the river bottom. The presence of woody debris is often associated with break-up. This interpretation is consistent

with the large amounts of woody debris found on SWIPS cable during the recovery of the Apr. 15 recovery operations

3.5 Sound Speed and Detection of Internal Ice Cover Structure/Composition

It is of interest to examine further the issue of sound speed in slush ice which, as noted in Section 3.3, directly impacts upon ice cover information extracted from SWIPS profile data. To clarify the interpretative uncertainties, roughly 13 days of profile data from Figure 3.3.2 have been replotted in Figure 3.5.1a,b,c with the range values of amplitudes associated with individual cells inside the ice cover alternatively “stretched”, “shrunk” or left unchanged to reflect different assumptions about ice cover sound speed. The upper panel (Figure 3.5.1a) is essentially a repeat of an early season portion of Figure 3.3.2 in that ice cover sound speeds are again set equal to the water column value. Figure 3.5.1b presents equivalent results based upon a slush sound speed of 2800 m/s or twice the freshwater speed value as would be expected from a fractional volume-weighted mean of the water and pure ice sound speed values. The resulting contrast with Figure 3.5.1a is dramatic and suggests that, under this increased speed alternative, SWIPS profile data returns would have been obtained throughout the entire ice layer.

The third plot (Figure 3.5.1c) was generated for slush sound speeds equal to 1000 m/s or 0.7 times the water sound speed value. This assumption is in accord with some preliminary laboratory and field experiments carried out with a downward-looking 307 kHz echosounder which measured time delays of acoustic returns from a target as a function of the fractional occupation by slush ice of an acoustic path which, otherwise pass through 0 °C water. The field results showed sound speed and attenuation to be sensitive to ice porosity and yielded a mean *in situ* speed estimate of 1100 m/s \pm 100m/s, slightly larger than the 1000 m/s \pm 50 m/s laboratory value obtained at a suspected slightly higher porosity (70% vs. 60%). Importantly, the field program was not successful in obtaining return signals for transmissions through the full depth of an approximately 50 cm slush layer, suggesting that the sound speed assumptions underlying Figures 3.5.1 a,b overestimate SWIPS profile penetration of the ice cover. The much more modest penetrations (equivalent to about 50% of the thickness of the depicted, still relatively “soft”, late-January-early February slush layer) suggested by the 1000m/s sound speed results (Figure 3.5.1c), thus, appear to be most in accord with current physical understandings.

Further quantitative exploitation of the SWIPS profiling mode for characterizing ice cover composition is likely to require both use of lower frequencies and knowledge of the dependences of sound speed and acoustic attenuation on ice properties such as porosity. Explanations of inferred slush sound speeds which are lower than those associated with either of the two major slush constituents may be found either in the complexities of the underlying ice-water interactions (Isakson and Chotiros, unpublished) or in extrinsic factors such as the presence of small concentrations of air bubbles (Commander and Prosperetti, 1989). Progress toward such explanations could enable quantitative characterization of internal portions of the consolidated ice layer and even allow acoustic monitoring of thermal ice draft values throughout the entire ice covered season.

4.0 Summary and Conclusions

The SWIPS provided valuable insights into numerous river ice processes involving: temporal and depth changes in suspended frazil ice concentrations; ice pan formation and growth; anchor ice growth and clearance; ice cover formation and evolution; effects of dynamic winter flow events; under-ice transport; and thermal break-up. Figure 3.3.1 summarizes the ice drafts for the entire Nov. – Apr. deployment period on a 12-hr statistical basis and provides a good overview of all the ice processes recorded by the SWIPS. Periods of scatter represented by the statistics indicate dynamic movement of ice or ice in suspension.

During the freeze-up process the SWIPS detected, within the first hour or two, occurrences of supercooling and the presence of frazil ice in suspension. The majority of the targets were concentrated in lower portions of the water column suggesting that the importance of interactions with the riverbed and/or its sediments in frazil ice nucleation. The observed decrease in the numbers of targets at higher levels in the water column implied that larger frazil flocs were fragmented into undetectable (i.e. smaller than 6 mm) particles by turbulence as they rose toward the river surface. It is recommended that a higher frequency SWIPS instrument be used to lower the minimum particle size detection threshold in future efforts to detect initial frazil ice formation.

Detection of sporadic surface ice floes by the SWIPS actually preceded initial detection of suspended frazil ice and the first evidence of supercooling near the river bed. The initial floes were typically 0.1 m or less in thickness. A sudden increase in the prominence of such floes was almost coincident with the first detection of frazil particles in the lower water column, approximately about 1 or 2 hours following supercooling. The SWIPS unit was able to document increases in the number, pan size (proportional to duration of feature detection) and thickness of the ice floes as the cold weather continued. These increases in surface coverage coincided with decreases in suspended frazil ice concentration in accord with theoretical expectations of greater isolation of the water column from atmospheric heat losses. Typical drafts of the frazil ice pans grew from about 0.2 m to 0.6 m, in rough agreement with estimates from video camera data which, because of logistical and anchor ice problems, did not coincide with a SWIPS data-recording period.

The formation of anchor ice on the SWIPS instrument was detected by the fading and eventual loss of the signal. Full losses of return signals were encountered in three separate time intervals associated with rapid cooling during freeze-up: with anchor ice clearance and resumption of signal reception following subsequent intervals of warmer temperatures. The occurrence of the final seasonal clearance of anchor ice during the period of ice cover formation suggests that insulation provided by an intact, complete, ice cover is sufficient to allow heat fluxes from the river bed to keep the SWIPS unit free of anchor ice. It is, however, recommended that future deployments include a heat source and/or a vibration mechanism to assure uninterrupted SWIPS measurement capabilities prior to ice cover formation. The fact that only the first anchor ice attachment interval produced physical displacements of the SWIPS unit was believed to be a consequence of the tightening of the unit's mooring cable by this initial movement. This result suggests that unit movements may be minimized and/or avoided by elimination of all cable slack during deployments. The periods associated with prominent frazil ice pans and anchor ice formation in the December-early January period preceding ice cover formation are readily

identified in Figure 3.3.1 from, respectively, their statistically higher scatter in draft values and by the simple absence of data.

The SWIPS record during the formation of the permanent winter ice cover provided valuable insights into the freeze-up consolidation process. The draft data from this period showed an initially relatively thin stabilized ice cover which was mobilized and stabilized again as a thicker ice cover before undergoing a third and largest consolidation. The latter consolidation produced the eventual stable winter ice cover at the monitoring site on Jan 7 about 16 hours after the initial consolidation event. It also contributed the largest ice draft (6.4 m) recorded during the entire ice season, corresponding to an ice feature which extended to within approximately 3 m of the river bed and the SWIPS unit. The observed maximum draft value was rather short lived as instantaneous drafts varied widely between high and low values during the consolidation event on time scales ranging upward from several seconds to almost a minute. The inferred presence of large draft features during the consolidation event is probably a consequence of local river geometry. This geometry (Figure 1.1.1) indicates that the initially wide Peace River narrows considerably just upstream of the SWIPS site as it passes the confluence with the Smoky River before widening again in the vicinity of the monitoring site. Thus, thickening would have been produced in the ice moving into the upstream constriction but subsequent expansion in the wider river near the SWIPS site would have introduced fissures and open water into thick conglomerated units of rubble ice and slush accounting for the highly variable draft values and large scale deep ice features seen in the SWIPS data record.

Once the ice stabilized after the Jan 7 event there was little change in the ice cover (other than gradual thinning) until Feb. 20. Nevertheless “apparent” changes were noted in the strengths of acoustic profile returns from the interior of the slush layer on time scales corresponding to several tens of minutes up to several hours. These changes (see for example, Figure 3.5.1) were, most likely, reflective of variability in the return acoustic paths caused by changes in the form of the slush ice undersurface (Section 3.3). Overall, the ice cover more or less went up and down with river levels accompanied by progressive, gradual, erosion of the slush layer. The profile data from the early part of the ice covered season suggested that the slush layer was characterized by, roughly, 0.1 to 0.2 m of softer ice, associated with weaker acoustic returns, at its lower interface. It may be beneficial to experiment with lower frequency SWIPS in the future to obtain greater penetration into the lower soft slushy layer to gain some insight into the internal more solid ice features in the frazil matrix or possibly detect the bottom of the thermal ice.

River flows increased towards the end of February and were substantially higher by Feb. 20. Between Feb. 20 and Feb. 23 the softer bottom layer of the slush ice almost disappeared with new targets appearing at depths down to 1 m below the slush-water interface on Feb. 23. Such targets continued to be present until the end of the mid-March flow event and were identified with suspended ice particles originating at or removed from the ice cover undersurface. These particles accounted for the increased scatter of draft values represented in Figure 3.3.1 for this period. Since the particle size detection limit for the SWIPS is about 6 mm, the sudden appearance of these targets suggests that either the transition from smaller particles (< 6 mm) to larger (> 6 mm) occurs rapidly through an, as yet, to be understood process, or that these larger particles were transported from upstream of the SWIPS site. Erosion rates of the slush layer increased during the high inflow Mar. 3 -15 event relative to earlier in the season.

The SWIPS record showed strong thinning of the ice cover prior to the arrival of the thermal break-up front, with the thinning rate increasing almost exponentially as the ice front approached to within 6 to 10 km of the SWIPS site. The cover load also increased at this time. The thinning rate then decreased, indicating that all slush below the thermal ice had melted. The SWIPS profiling clearly showed this step to be accompanied by the disappearance of the weak returns previously associated with the near (short range) edge of the profile signal. The subsequent sharp rise in amplitude at this edge was identified as a characteristic signature of the bare thermal ice undersurface. The denser and smoother thermal ice slowed down further melting through its greater heat input requirements and less favourable heat transfer properties. Break-up was uneventful and the measured ranges were equal to those of the water surface on Apr. 3 (Figure 3.4.2). There was however a larger amount of scatter in ice targets for 2 days following break-up due to detection of pieces of drifting, recently released, shore ice. Some woody debris near the bed was also detected by the SWIPS during this period.

In summary, over the course of the ice season, the SWIPS instrument provided a wealth of insights into river ice processes. Future deployment of the unit at the Peace River site as well as on other rivers should both advance knowledge of river ice processes significantly and provide realtime monitoring capabilities. The continuing collection of SWIPS data on the Peace River will be helpful in calibrating river ice models and assessing frazil ice transport and deposition and how the Dunvegan Project could change these processes and therefore also ice management practices on the Peace River.

Acknowledgments

The participation of the Town of Peace River for the use of their water treatment plant pumphouse to provide shelter and power for the SWIPS data logger is greatly appreciated. SWIPS development and testing was carried out by Matt Stone and Bob Lane of ASL Environmental Sciences. SWIPS deployment was carried out by Matt Stone, and assisted by Kerry Paslawski, Timberroot Environmental, Chandra Mahabir, Evan Friesenhan and Gordon Fonstad, Alberta Environment. Field data collection was assisted by Bruce Smiley and Frank Weber, BC Hydro, Evan Friesenhan, Alberta Environment. SWIPS retrieval was carried out by Timberroot Environmental and Willi Granson, Alberta Environment. John Kramer supplied the jet boat and driving skills for SWIPS deployment and retrieval.

Ice front locations, aerial ice observations and water level surveys at the SWIPS site were provided (Willi Granson, Gordon Fonstad, and Evan Friesenhan, Alberta Environment). Lorraine Crist, Bob Hill, Glenn McTaggart, Wayne Smith, Darin Thompson, BC Hydro also provided ice front locations and aerial ice observations. SWIPS data post-processing was performed by Vincent Lee, Ed Ross and Matt Tradewell, ASL Environmental. David Lemon and Rene Chave, of ASL Environmental as well as Dr. Humfrey Melling of DFO, participated in helpful discussions on underwater acoustic issues. Environment Canada provided water level and meteorological data.

References

Andres, D. (1995) Floe Development During Frazil Generation in Large Rivers, 8th Workshop on the Hydraulics of Ice Covered Rivers, Kamloops.

Andres, D., Van Der Vinne, G. (2004), Summary of Observations of Ice Conditions on the Peace River, 2002-2003 & 2003-2004. A report prepared by Trillium Engineering and Hydrographics Inc. for Glacier Power Ltd.

Birch, R., Fissel, D., Melling, H., Vaudrey, K., Schaudt, K., Heideman, J., and Lamb, W., 2000. Ice Profiling Sonar – Upward looking sonar provides over-winter records of ice thickness and ice keel depths off Sakhalin Island, Russia. *Sea Technology* – Aug. 2000 issue, pp. 35 to 41.

Chacho, E.F., Lawson, D.E., Brockett, B.E. (1986) Frazil pebbles: frazil aggregates in the Tanana River near Fairbanks, Alaska. *Proceedings of the 8th IAHR Ice Symposium, August 1986, Iowa City, vol. I pp. 475-484.*

Chave, R.A.J., D.D. Lemon, D.B. Fissel, L. Dupuis and S. Dumont, 2004. Real-Time Measurements of Ice Draft and Velocity in the St. Lawrence River *Proceedings of Oceans 2004 Conference, Kobe, Japan. IEEE Press.*

Commander, K.W. and A. Prosperetti, 1957. Linear Pressure waves in bubbly liquids: Comparison between theory and experiments. *J. Acoust. Soc. Am.* **85**, pp 732-746]

Daly, S.F. and R. Ettema, 2005. Monitoring for Frazil Ice Accumulation on Freshwater intakes in the Nearshore Zone, *Proceedings of the 18th International Conference on Port and Ocean Engineering under Arctic Conditions (POAC '05), Potsdam, N.Y, pp 805-814.*

Fissel, D.B., J.R. Marko and H. Melling, 2004. Upward Looking Ice Profiler Sonar Instruments for Ice Thickness and Topography Measurements. In: *Proceedings of Oceans 2004 Conference, Kobe Japan, Nov. 10-12, IEEE Press. 6 p.*

Granson, W., Friesenhan, E. and Fonstad, G. (2005a) Alberta Environment – Ice Observation Report #33.

Granson, W., Friesenhan, E. and Fonstad, G. (2005b) Alberta Environment – Ice Observation Report #9.

Lal, A.M. W. and Shen H.T. (1991) A Mathematical Model for River Ice Processes, *Journal of Hydraulic Engineering.*, ASCE, 117(7), 851-867 Also CRREL Report 93-4

Melling, H., P.H. Johnston and D.A. Reidel, 1995. Measurement of the draft and topography of sea ice by moored sub-sea sonar, *J. Atm. Oceanic Tech.*, 13, pp. 589-602.

Morse, B., Hessami, M., Bourel, C., (2003) Characterization of ice in the St. Lawrence River. *Canadian Journal of Civil Engineering.* No. 30, pp. 766-744.

Neill, C.R., Yaremko, E.K., Van Der Vinnie, Andres, D.D. (1995) Under-ice hydraulics and mixing in regulated rivers. Proceedings of the 8th Workshop on the Hydraulics of Ice Covered River, Kamloops, BC.

Shen, H. T, Yapa, P. D. (1985) A Unified Degree-Day Method for river ice cover thickness simulation, Canadian Journal of Civil Engineering Vol. 12, pp54-62.

Shen, H.T. and Wang, D. (1995) Undercover Transport and Accumulation of Frazil Granules Journal of Hydraulic Engineering, ASCE, 121 (2),184-195.

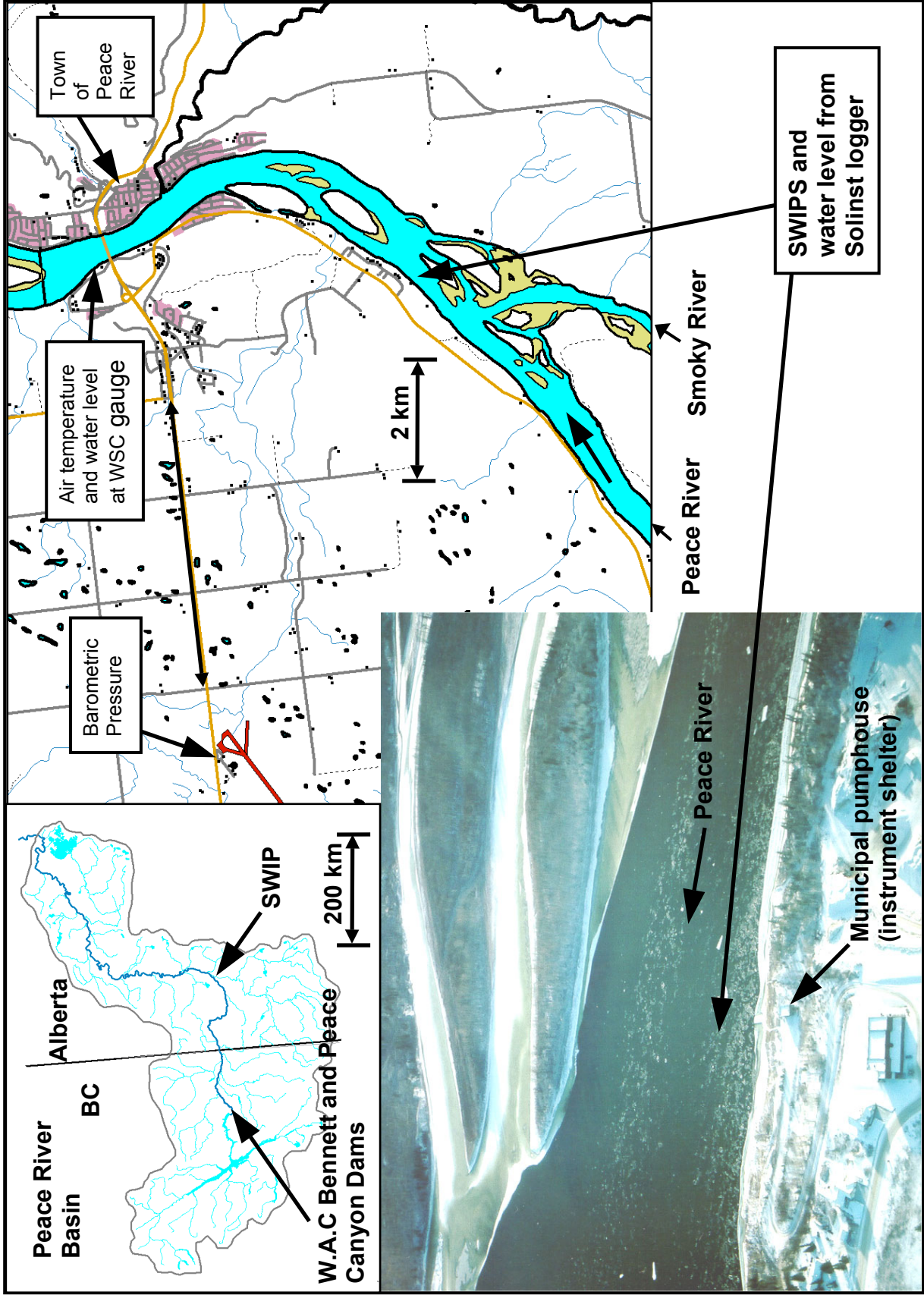


Figure 1.1.1 Geographic location of SWIPS unit and meteorological stations.

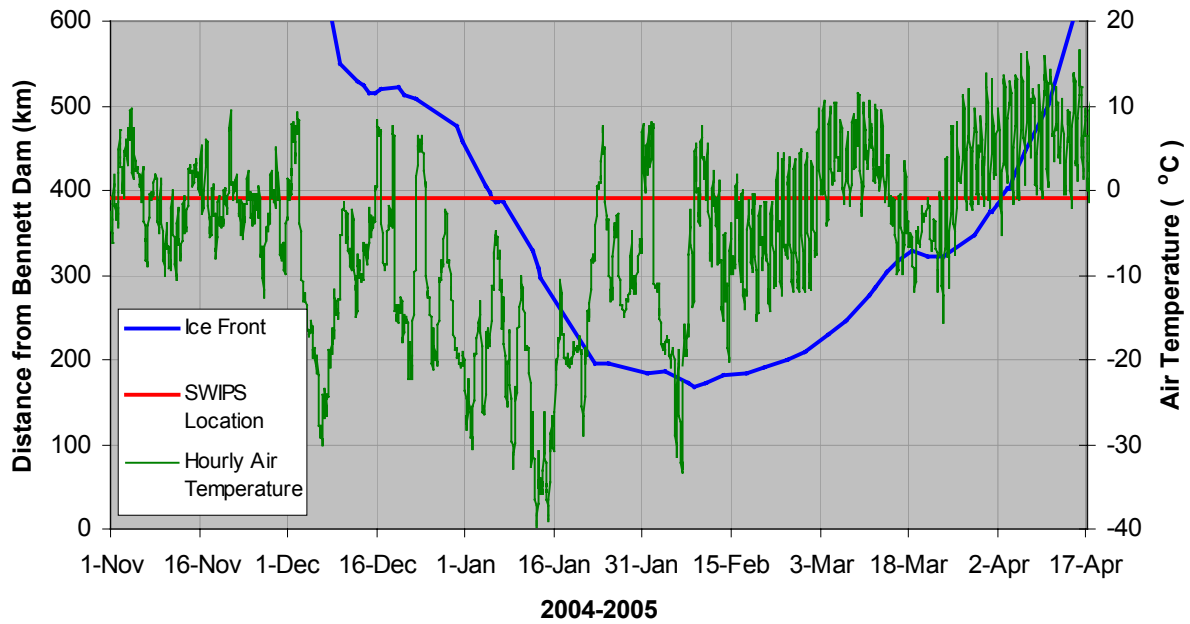


Figure 1.2.1 Location of SWIPS, ice front and hourly air temperature at the Town of Peace. (Stationary ice cover present above blue line)

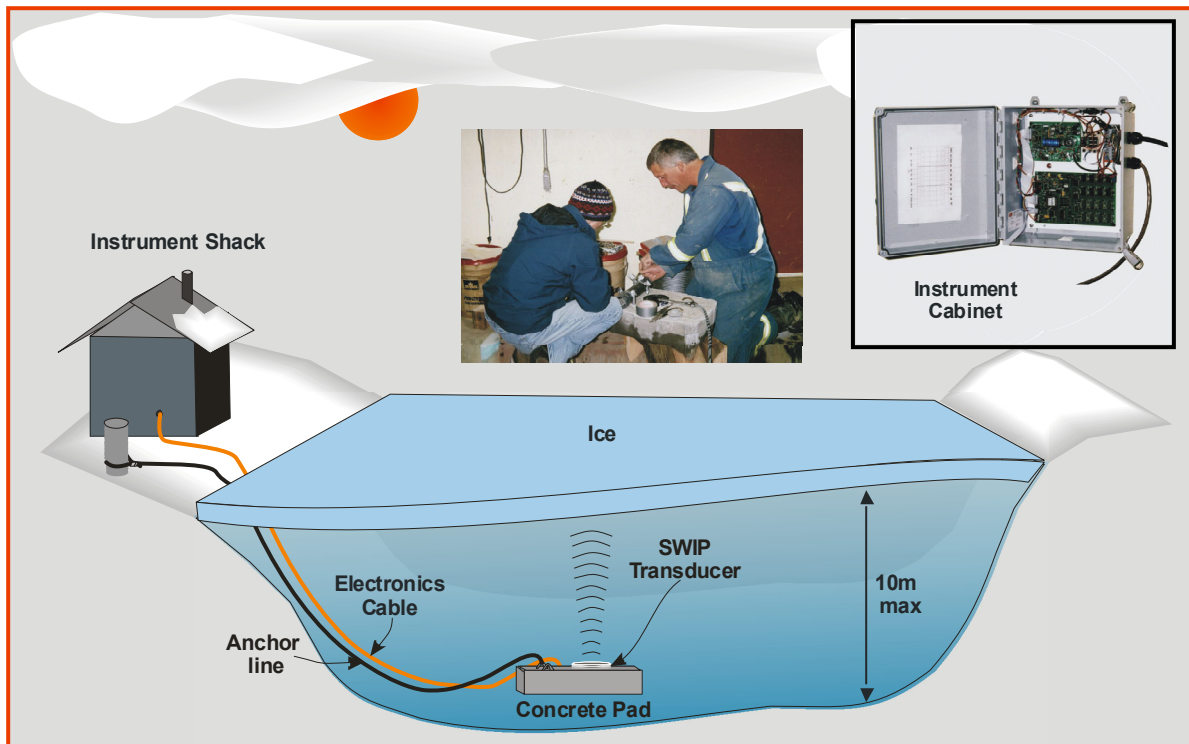


Figure 2.1.1 SWIPS unit and data logger installation.

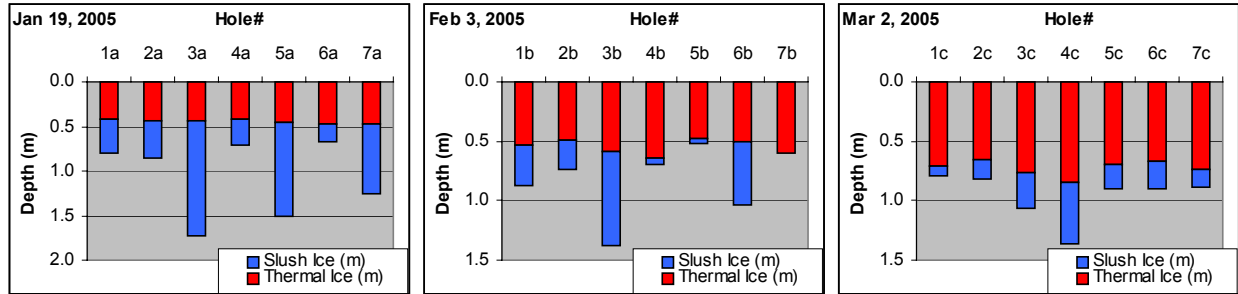


Figure 2.1.2. Thermal, slush and total ice thicknesses measured near the SWIPS site.

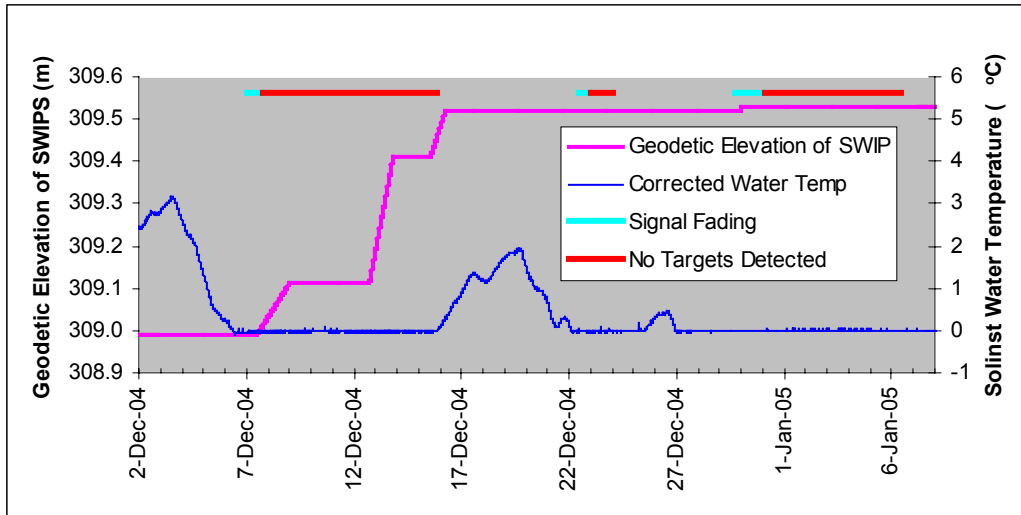


Figure 3.1.1a SWIPS geodetic elevation and water temperature at times before, during and after December movement.

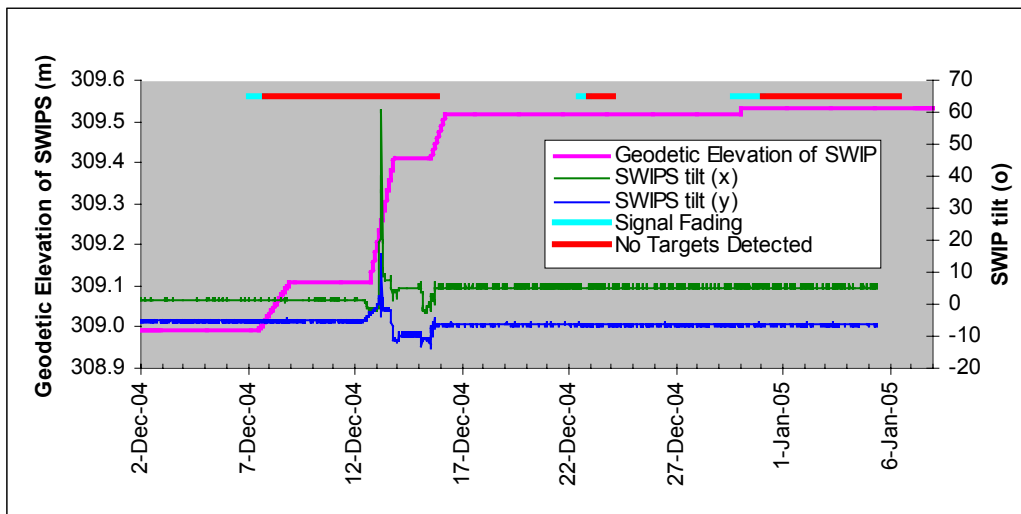


Figure 3.1.1b SWIPS geodetic elevation and x- and y-axes tilt before, during and after December movement.

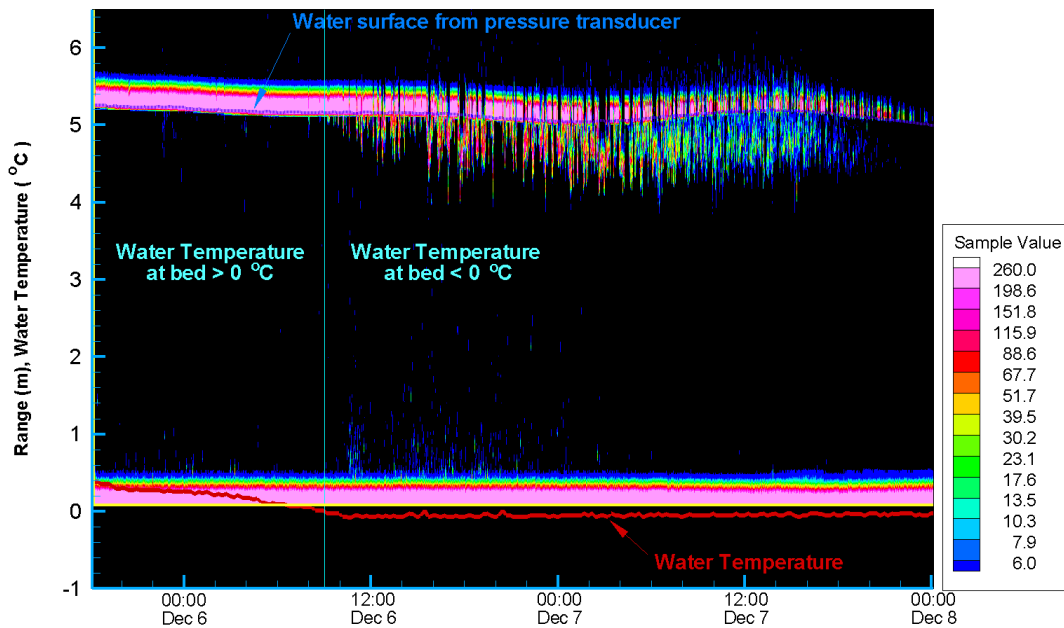


Figure 3.1.2 SWIPS profile data, water temperature and water level for Dec. 6-7, 2004 when water temperature at the bed first went below freezing.

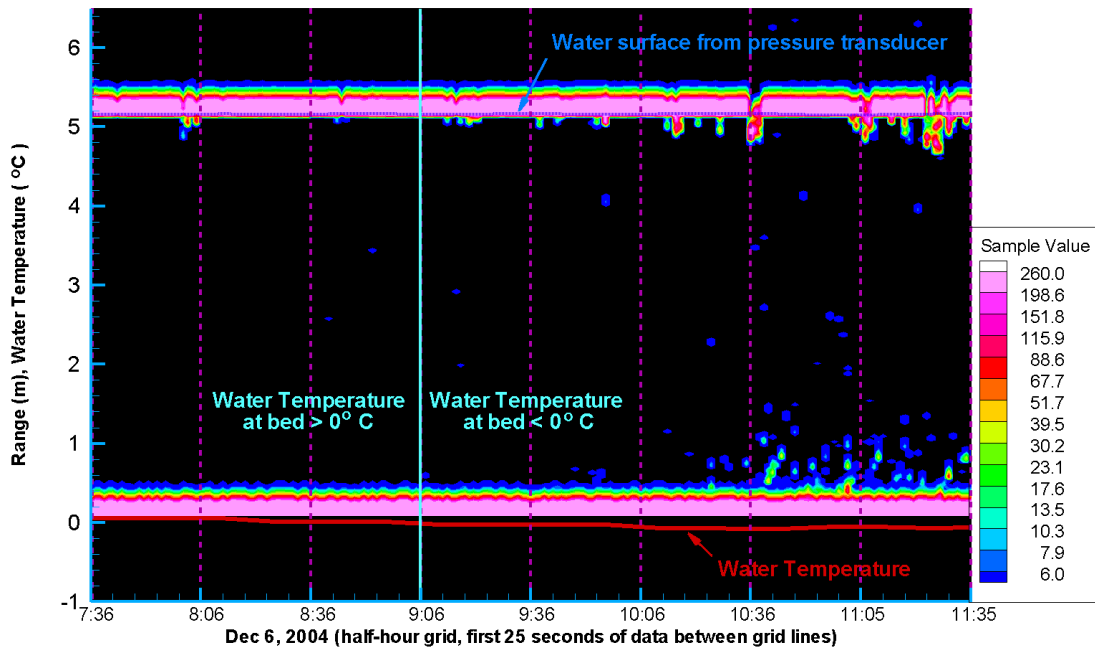


Figure 3.1.3a Dec. 6, 2004 SWIPS 1-second resolution profile data for 25 seconds as recorded at half hour intervals denoted by the vertical grid lines. A small number of floe targets with drafts < 0.25 m are evident along with suspended ice concentrated in the lower water column. Water temperatures and water level are also shown along with the timing of the initial drop of bed temperatures below the freezing point.

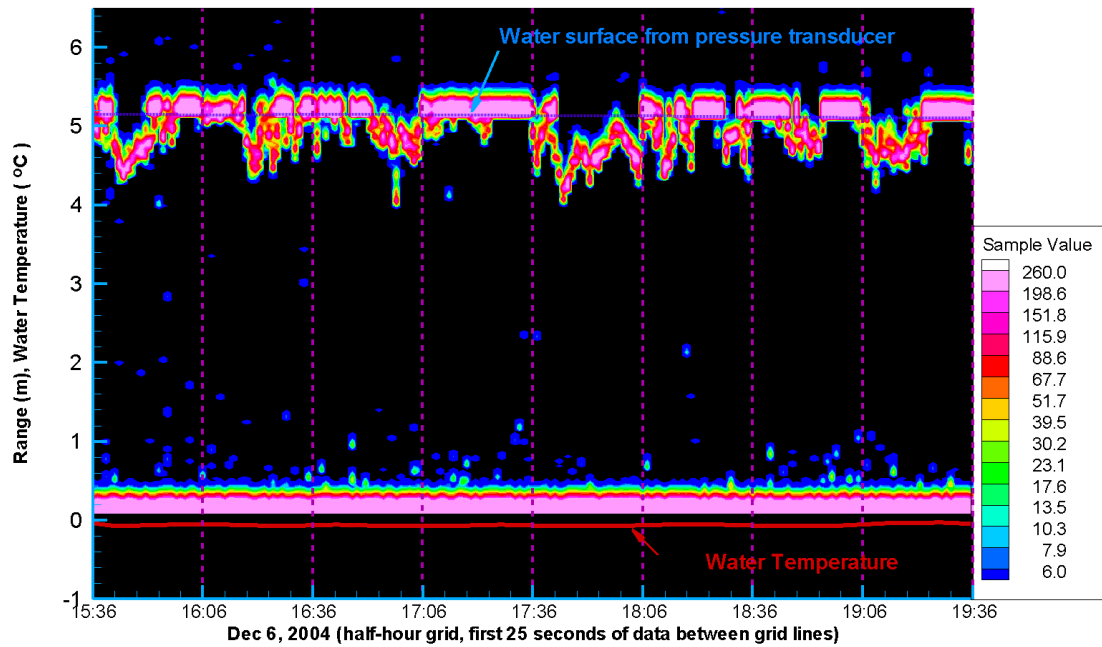


Figure 3.1.3b Dec. 6, 2004 SWIPS 1-second resolution profile data for 25 seconds as recorded at successive half-hour intervals denoted by vertical grid lines. Floes are seen in high concentrations with maximum drafts as large as 1 m. Also shown are water temperatures and water levels.



Figure 3.1.4 Frazil ice pans on the Peace River.

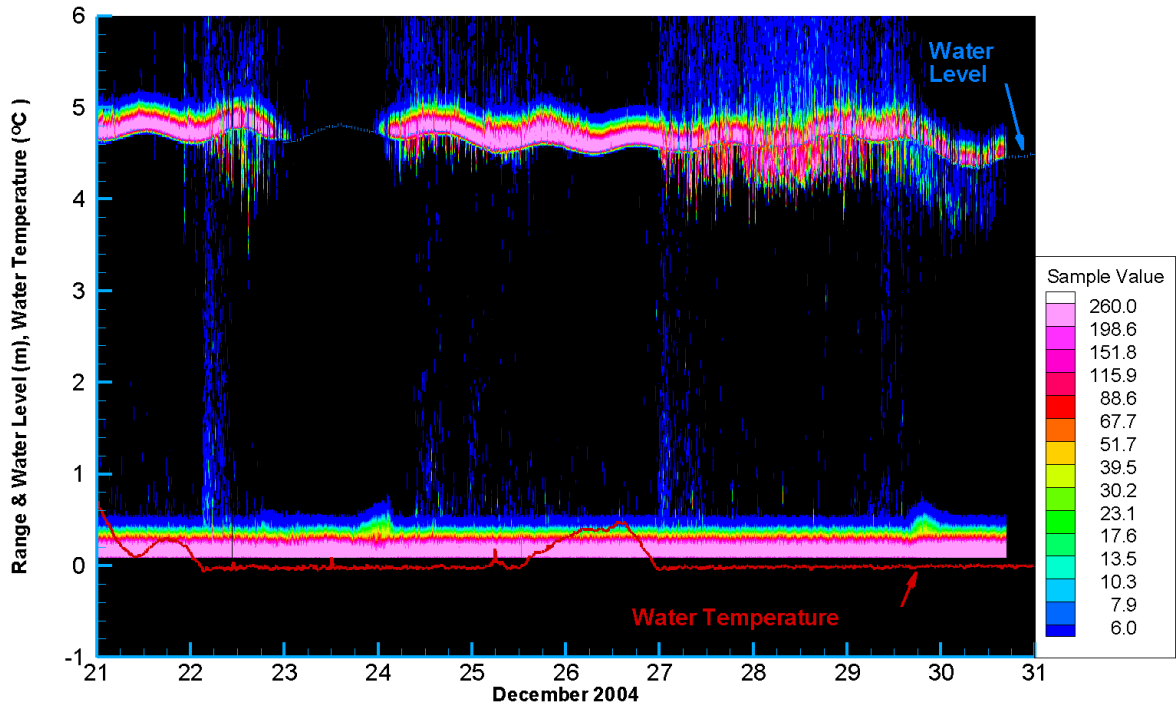


Figure 3.1.5a Profile data, water level, and water temperature Dec. 21 to 30, 2004.

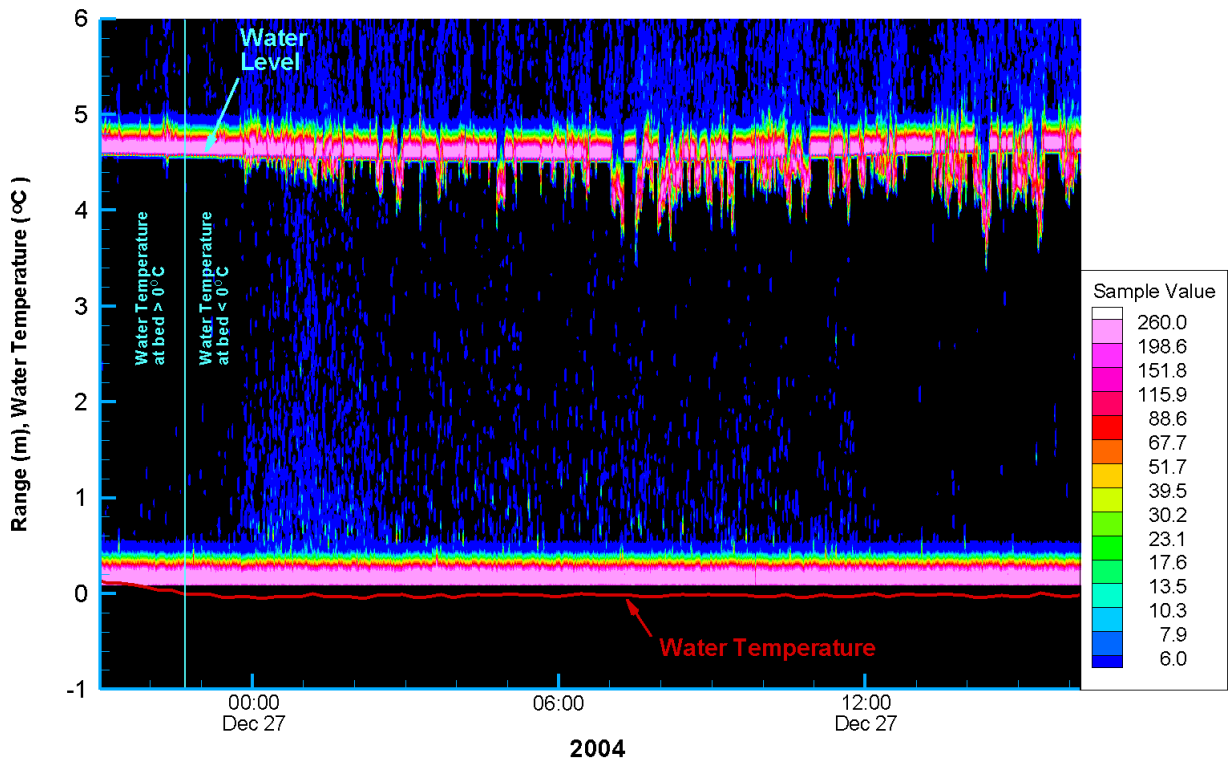
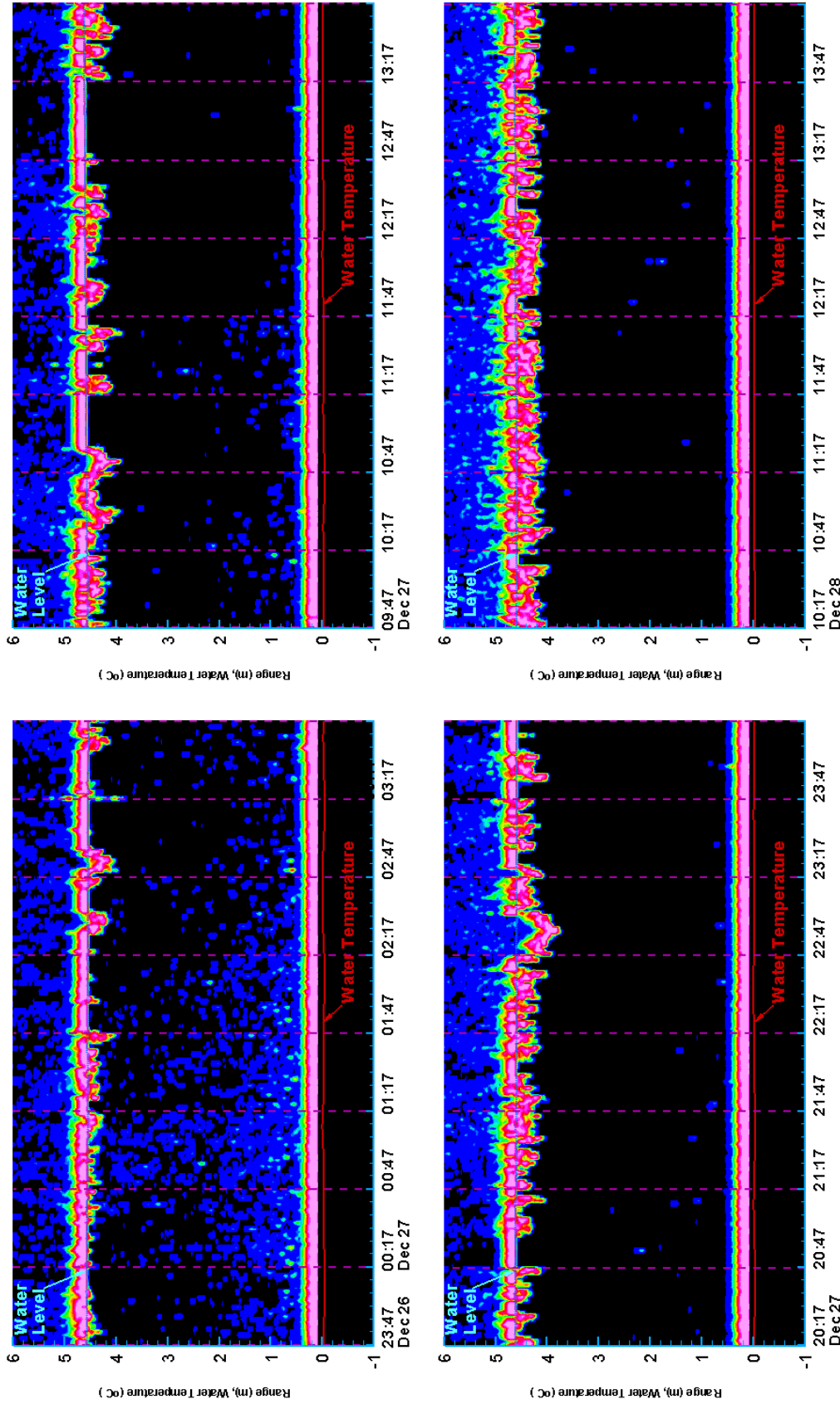


Figure 3.1.5b Profile data, water level, and water temperature Dec. 26-27, 2004.



December 26-28, 2004 (3.5 hr windows, half hour grid, first 25 seconds of data between grid lines)

Figure 3.1.5c 1 second resolution profile data, water level, and water temperature for four 3.5 hour windows during Dec. 26-28, 2004. Air temperatures were -15 to -20 °C during this time.

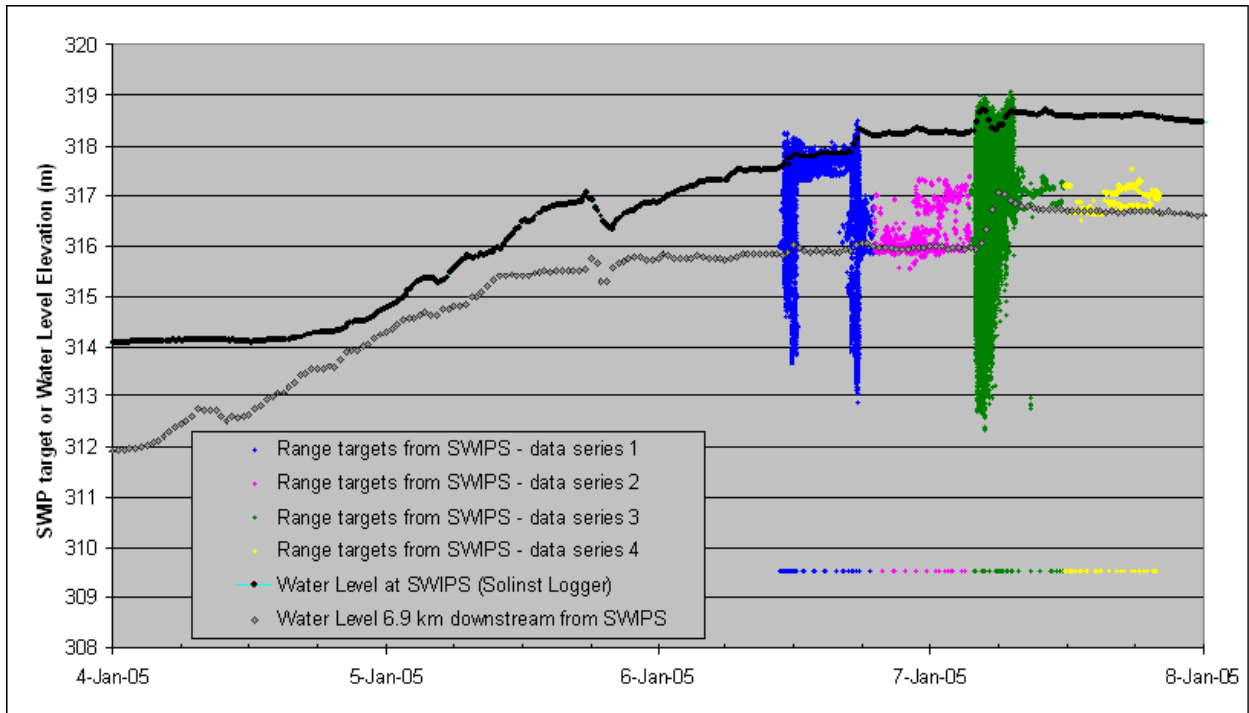


Figure 3.2.1 SWIPS target and water levels with respect to geodetic elevation during ice cover formation period. Anchor ice broke free from unit on Jan. 6, 09:56 and three subsequent ice consolidation movements were recorded. The largest of which was on Jan 7.

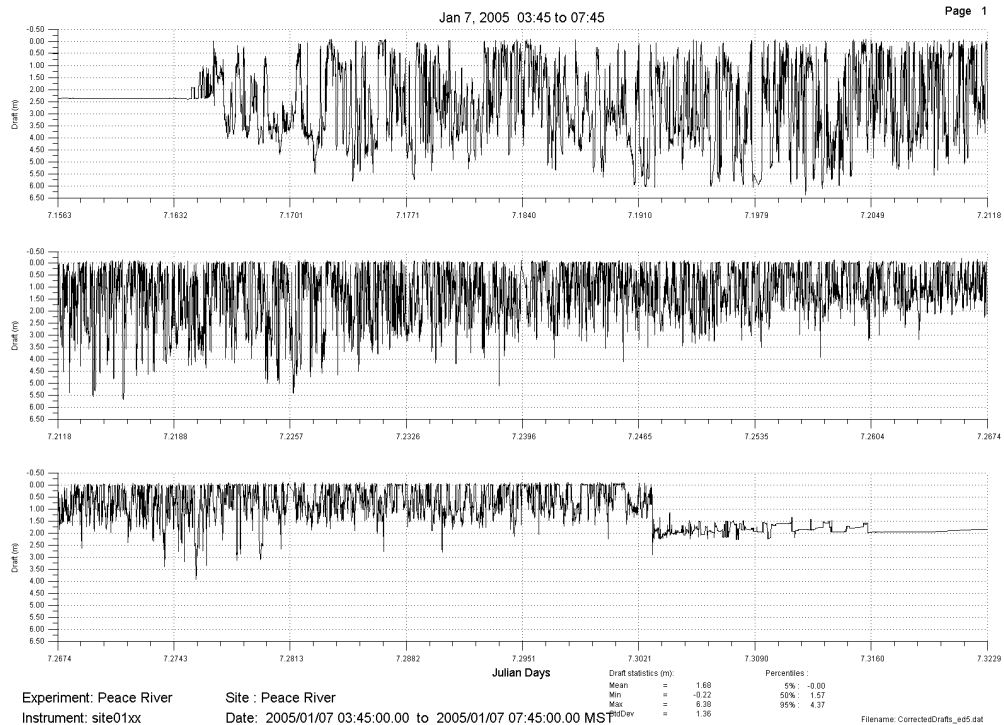


Figure 3.2.2 Ice draft during Jan. 7 consolidation event.

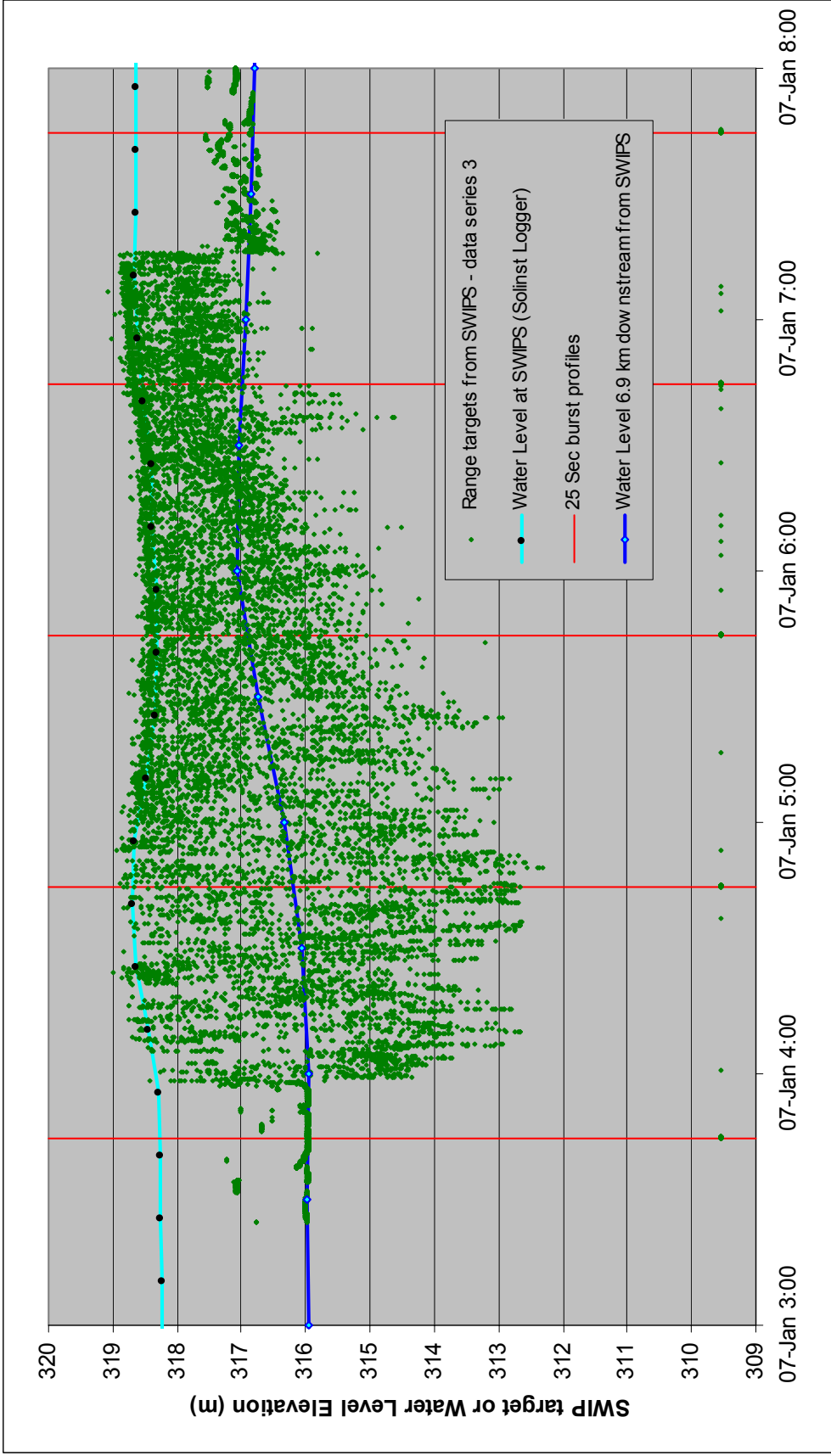


Figure 3.2.3 SWIPS target and water levels with respect to geodetic elevation during major consolidation event on Jan. 7. Times for the 25 sec profile data are also shown.

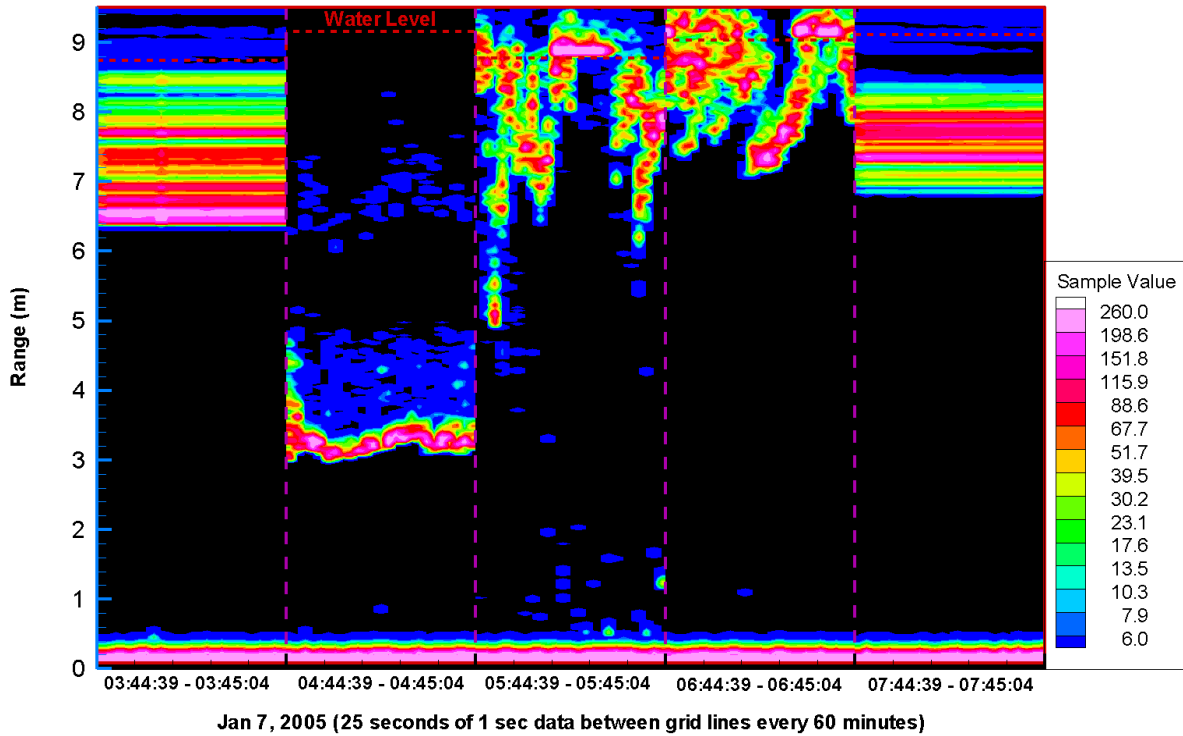


Figure 3.2.4 Profiles before during and after major consolidation movement on Jan. 7. Times for these are also shown in Figure 3.2.3.

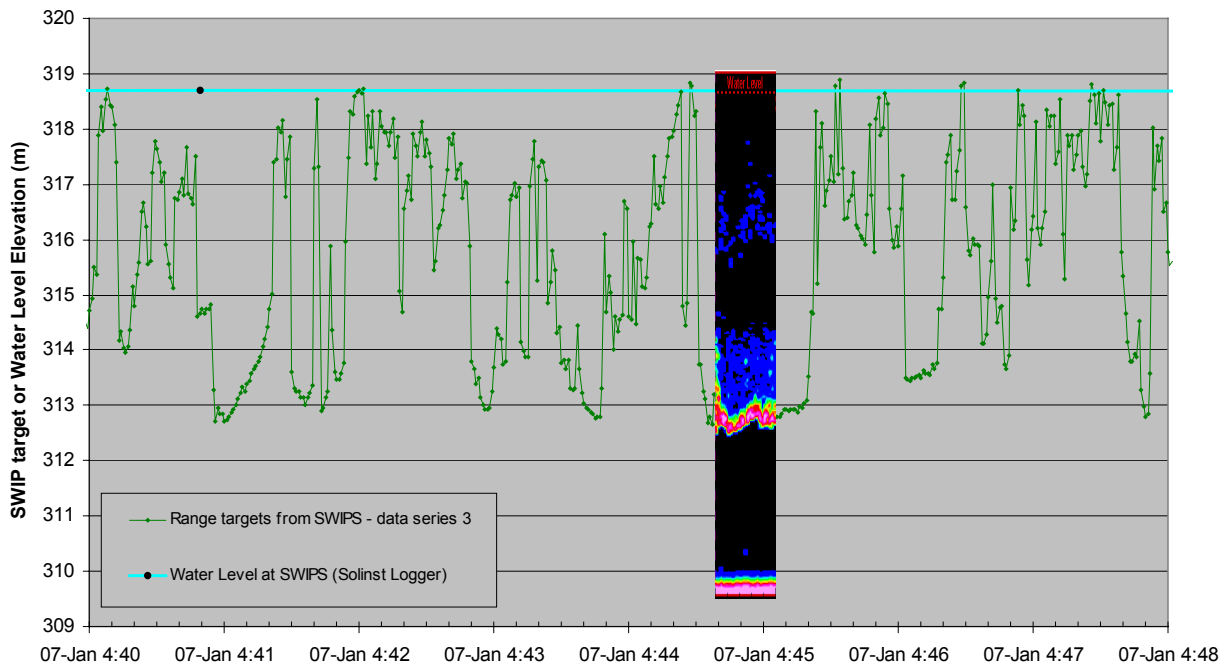


Figure 3.2.5 SWIPs target and water levels with respect to geodetic elevation during the major consolidation event on Jan. 7 associated with the thickest portions of the observed ice run. Also shown are 25 seconds of SWIPs profile data coincident with a portion of this data record.

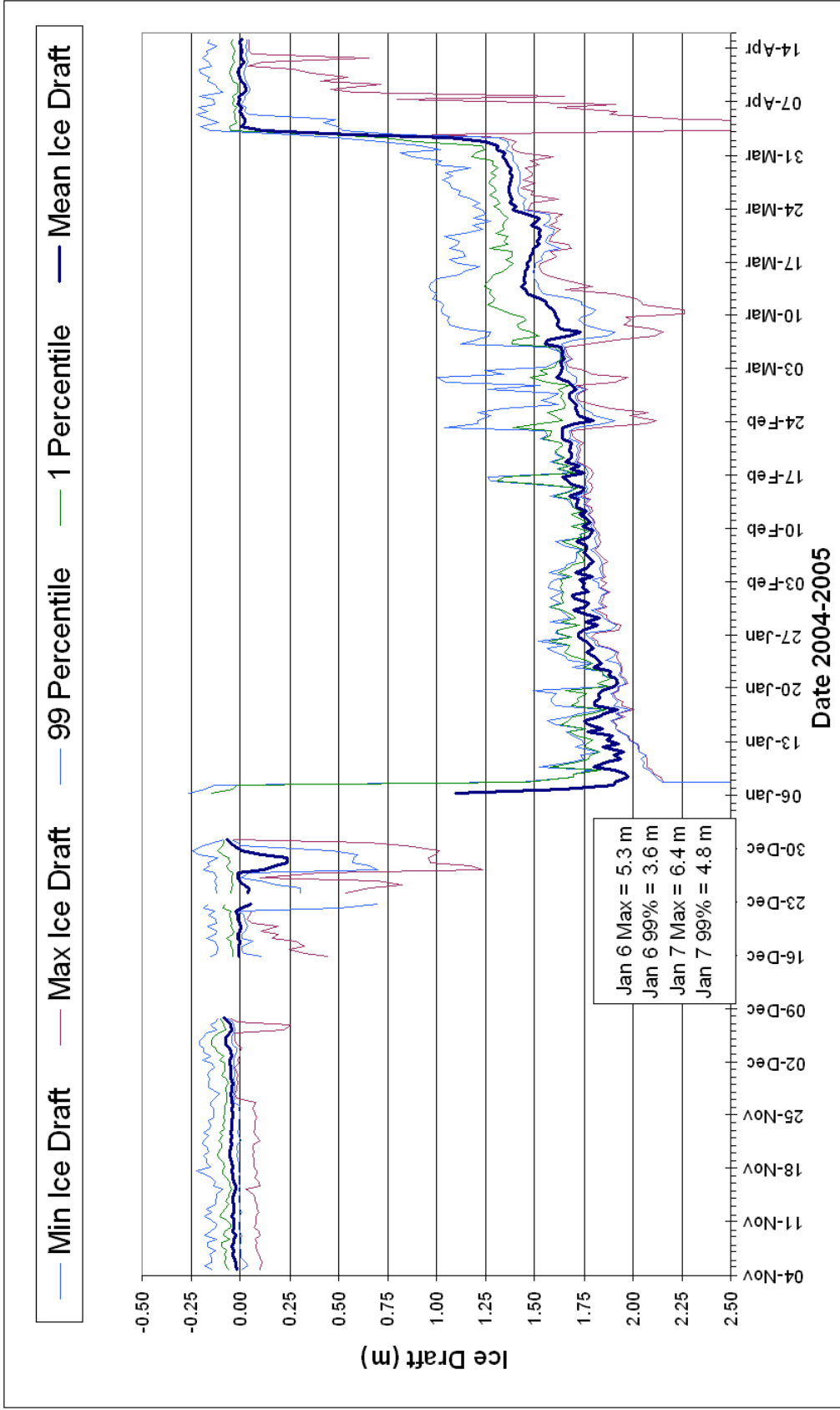


Figure 3.3.1 Ice Draft statistical values derived from the continuous 1 Hz SWIPS target range measurements, and computed at 12 hour intervals from Nov. 4, 2004 to Apr. 15, 2005.

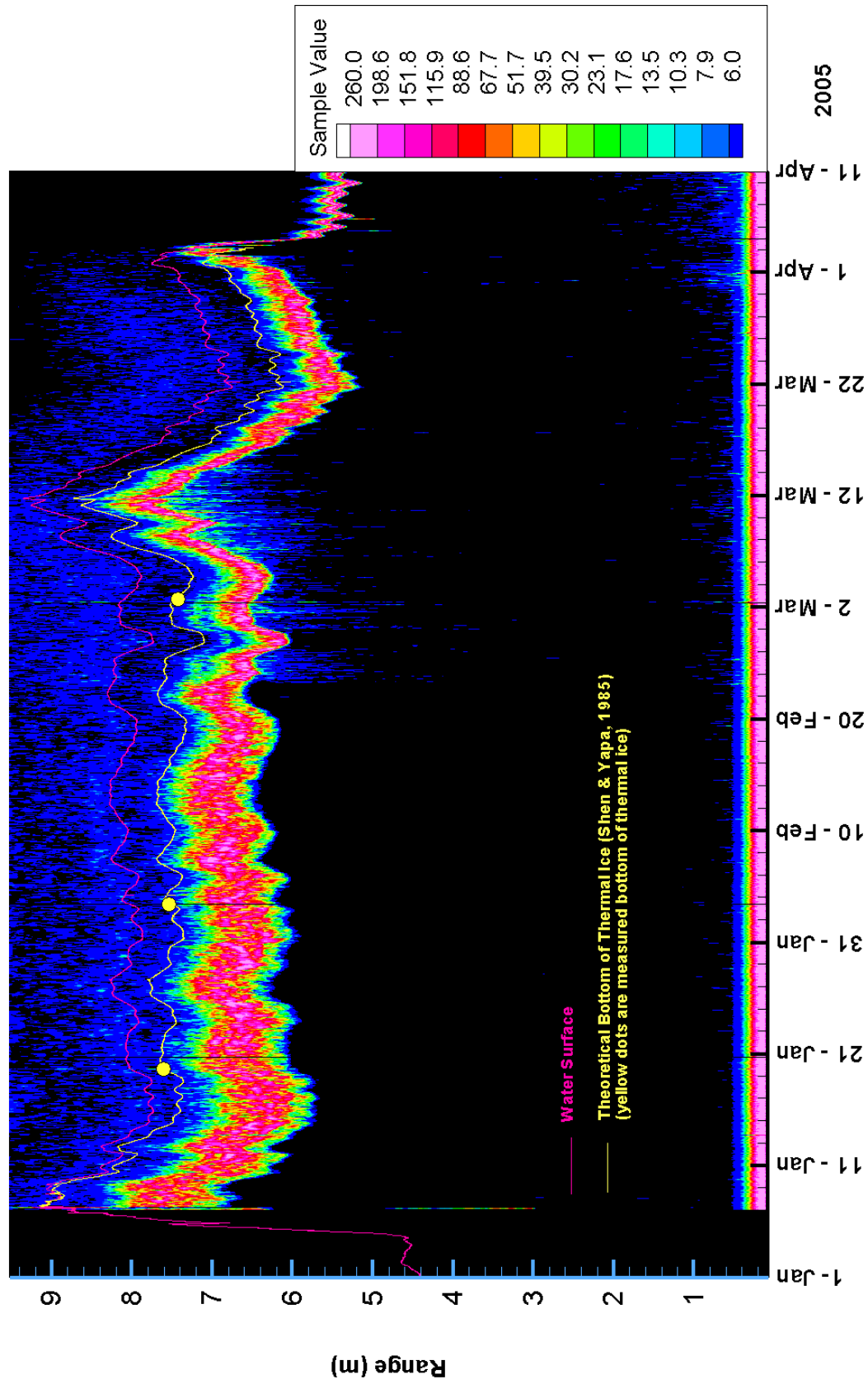


Figure 3.3.2 Hourly profiles for mid-winter stationary ice covered period Jan. - Apr. Thermal break-up occurred on Apr. 3. Also shown are the water level, the theoretical bottom of thermal ice and measured bottom of thermal ice for 3 dates.

Selected Amplitude Profiles Averaged Over 12 Hours

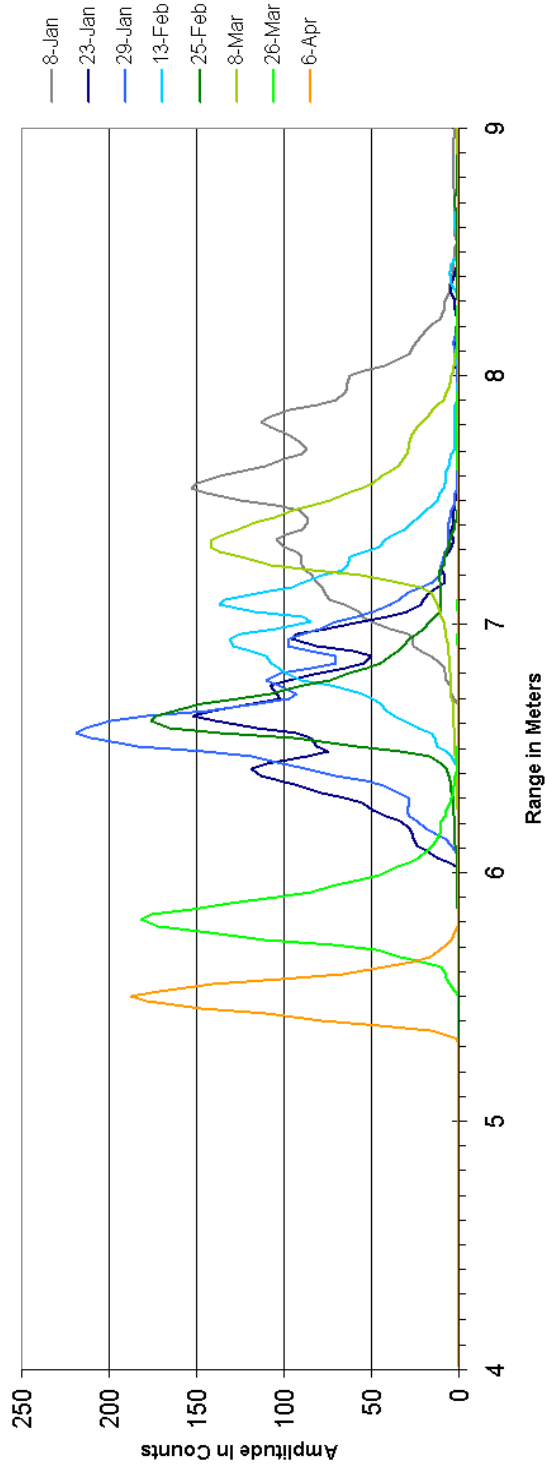


Figure 3.3.3 Amplitude profiles averaged over 12 hours for different times during the ice season.

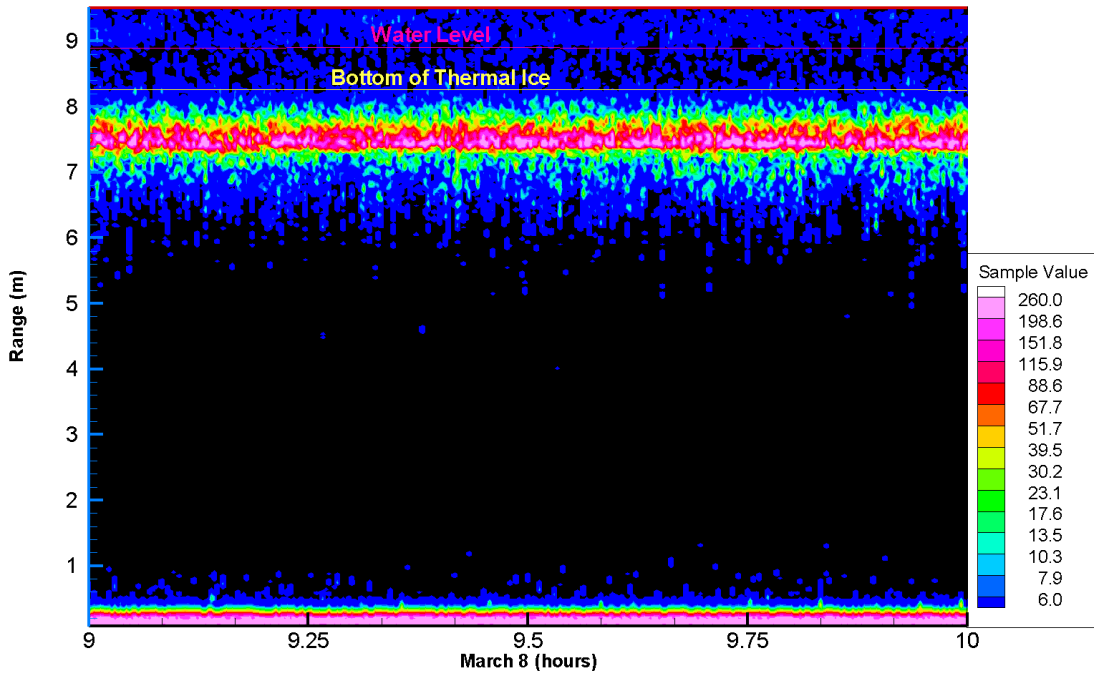


Figure 3.3.4 12-sec profile data on March 8, 2005 showing undercover ice transport.

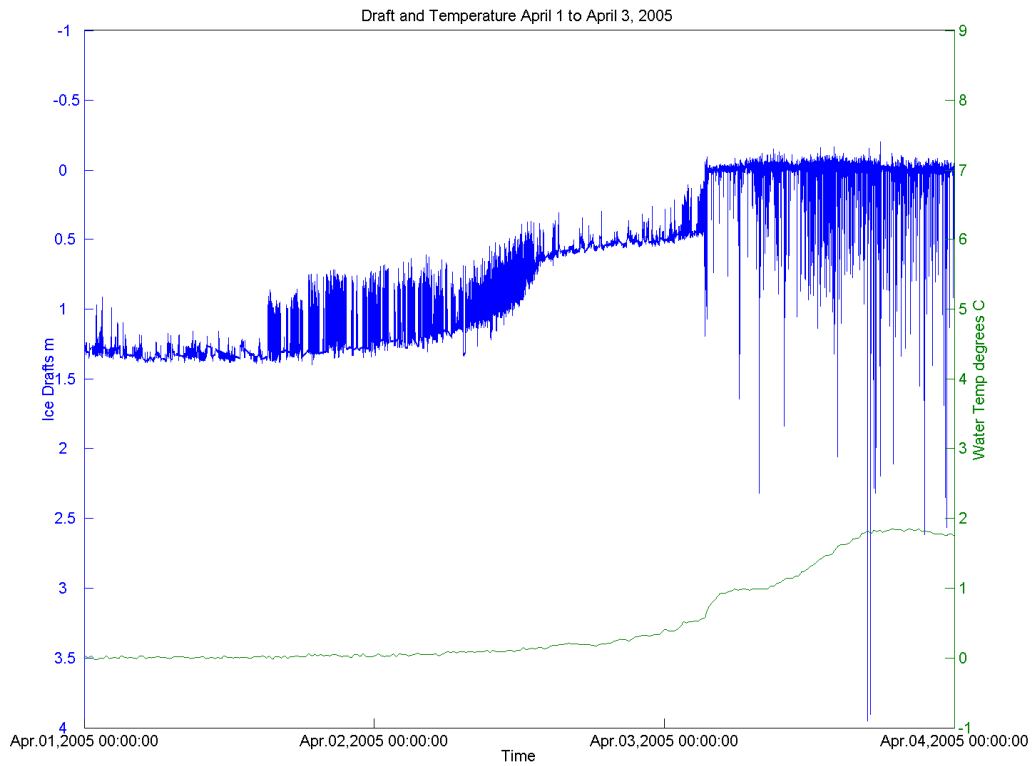


Figure 3.4.1 Ice draft and water temperature during thermal break-up period Apr. 1-3, 2005.

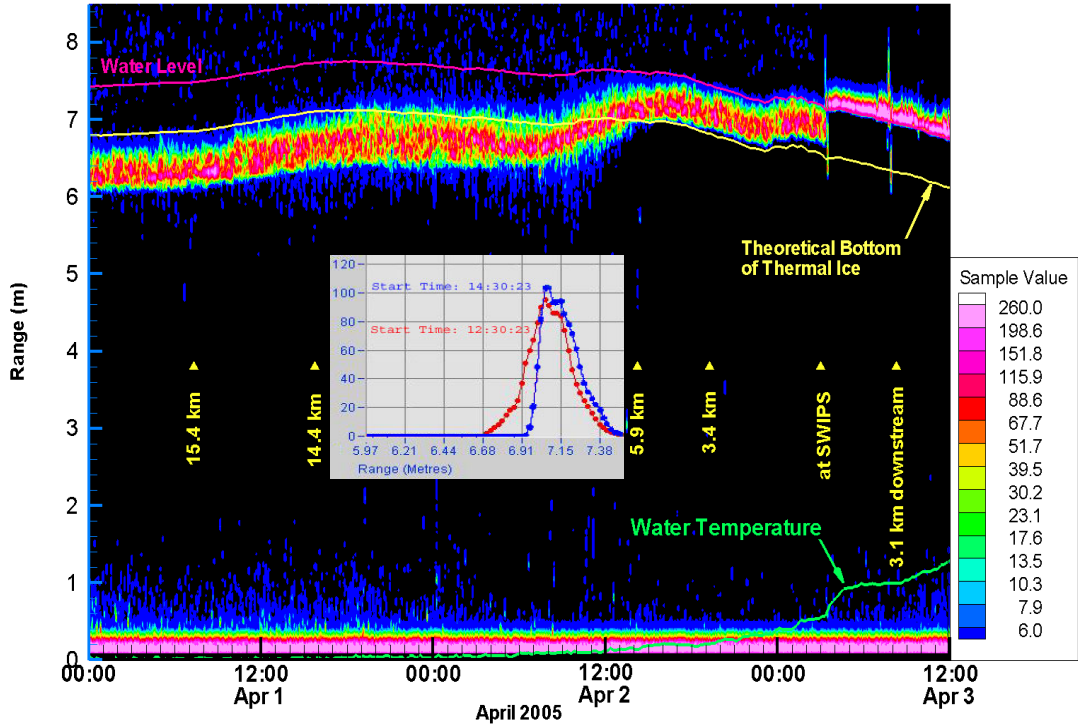


Figure 3.4.2 Five minute profile data, showing water temperatures, water levels and the theoretical positions of the bottom of the thermal ice for times close to break-up (at approximately 03:24, April 3). Distances to the ice front location from the SWIPS site are shown (as vertical labels) for various times. The inset figure displays thirty minute mean amplitude profile plots for times starting 0.5 hours before (red curve) and 1.5 hours after (blue curve) the approximately 14:00 April 2 initial merging of the detected ice under-surface and the bottom of the thermal ice.

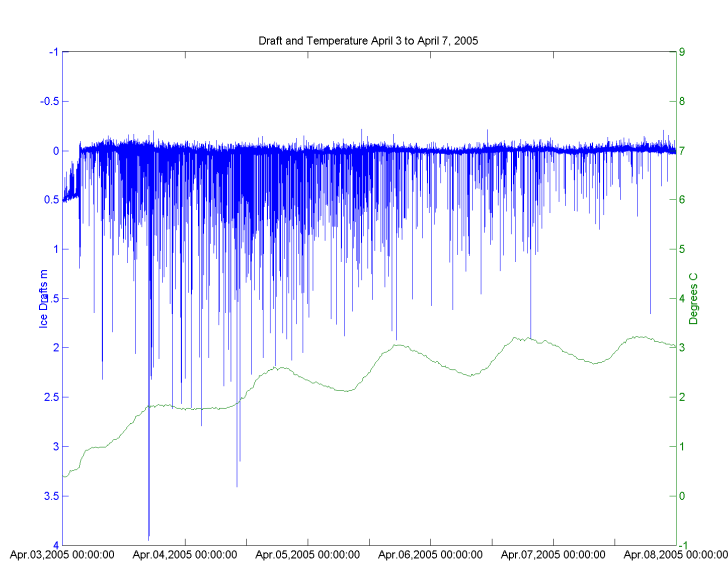


Figure 3.4.3 Ice draft and water temperature Apr. 3-7, 2005 following thermal break-up period.

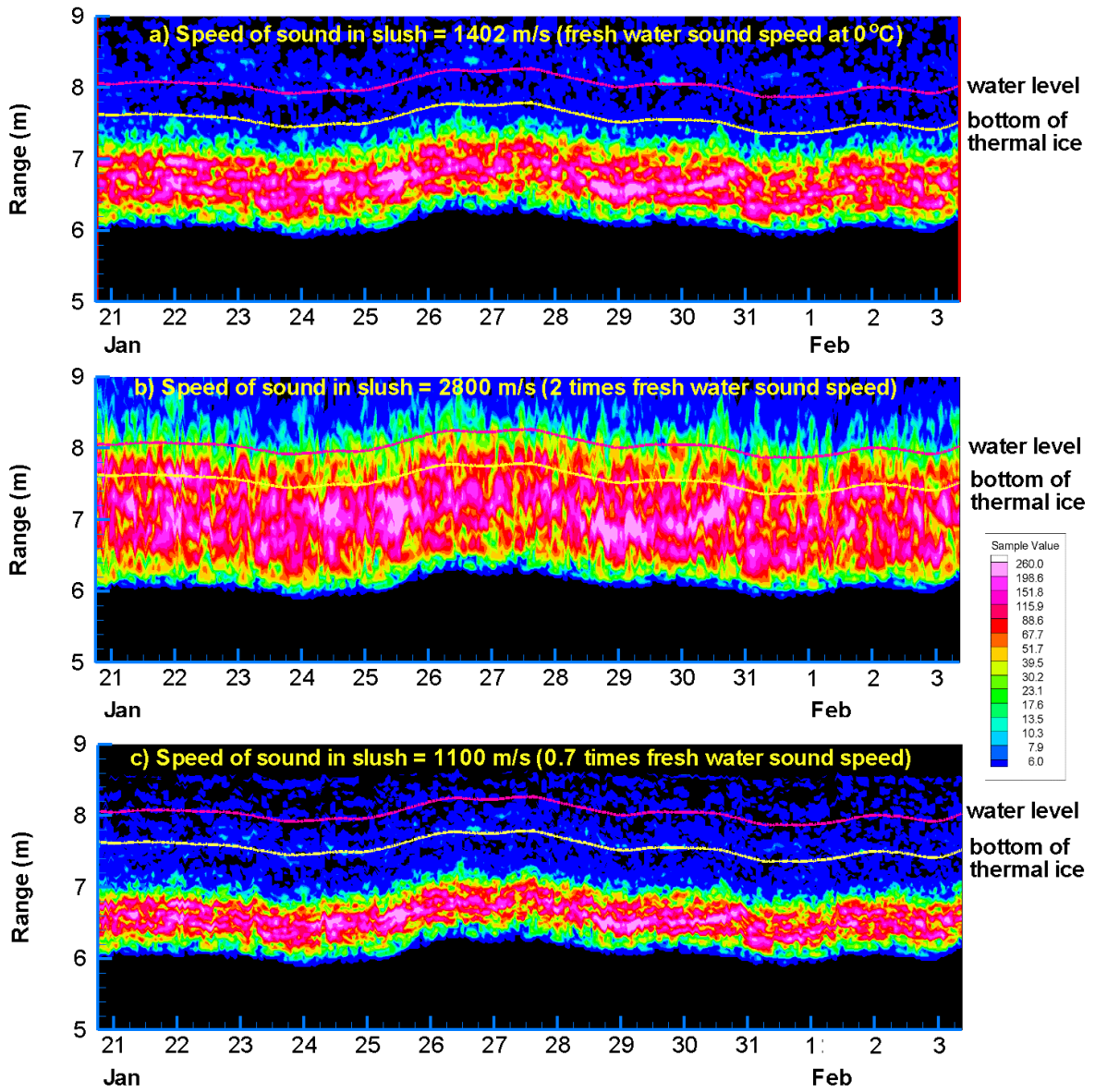


Figure 3.5.1 Profiles with range values of amplitudes associated with individual cells inside the ice cover alternatively “stretched”(b), “shrunk” (c) or left unchanged (a) to reflect different assumptions about ice cover sound speed.